NASA TECHNICAL MEMORANDUM

NASA TM-77786

RESEARCH DONE AT D.E.R.A.T. (OCTOBER 1982 THROUGH SEPTEMBER 1983); SUMMARY OF PRINCIPAL RESULTS OBTAINED

None Given

Translation of "Recherches effectues au D.E.R.A.T. (Octobre 1982 a Septembre 1983); Bilan des principaux resultats acquis. O.N.E.R.A. Centre d'Etudes et de Recherches de Toulouse, Toulouse, France, October 17, 1983, pp. 1-42

NATIONAL AERONAUTICS AND SPACE ADMINISTRATION
WASHINGTON D. C. 20546 DECEMBER 1984

STANDARD TITLE PAGE

1. Report No. NASA TM-77786	2. Government Accession No.	3. Recipient's Catalog No.
4. Title and Subtitle RESEARCH DONE AT D.E.R.A.T. (OCTOBER 1982 THROUGH SEPTEMBER 1983); SUMMARY OF PRINCIPAL RESULTS OBTAINED		5. Report Date December, 1984 6. Performing Organization Code
7. Author(s) None Given		8. Performing Organization Report No. 10. Work Unit No.
9. Performing Organization Name and Address SCITRAN Box 5456 Santa Barbara, CA 93108		11. Contract or Grant No. NASw- 4004 13. Type of Report and Period Covered Translation
12. Sponsoring Agency Name and Address National Aeronautics and Space Administration Washington, D.C. 20546		14. Sponsoring Agency Code

15. Supplementary Notes
Translation of "Recherches effectues au D.E.R.A.T. (Octobre 1982 a Septembre 1983); Bilan des principaux resultats acquis. O.N.E.R.A. Centre d'Etudes et de Recherches de Toulouse, Toulouse, France, October 17, 1983, pp. 1-42

16. Abstract
The progress in the following areas is described: measurement equipment, F2 FAUGA wind tunnel tests, unsteady boundary layers, body and axisymmetrical boundary layers, wing fuselage interactions, turbulence, subsonic-transonic flow, cryogenic wind tunnel tests, profile testing.

17. Key Words (Selected by Author(s))	18. Distribution Statement
	Unclassified and Unlimited

19. Security Classif. (of this report)	20. Security Classif. (of this page)	21. No. of Pages	22. Price
Unclassified	Unclassified	79	

ONERA

CENTRE D'ETUDES ET DE RECHERCHES DE TOULOUSE

(TOULOUSE CENTER FOR STUDIES AND RESEARCH)

2 Avenue Edouard Belin - 31055 TOULOUSE CEDEX - FRANCE

B.P.4025 - TELEPHONE (61)55 71 11

DEPARTEMENT D'ETUDES ET DE RECHERCHES EN

AERODYNAMIQUE (D.E.R.A.T.)

(DEPARTMENT FOR STUDIES AND RESEARCH IN AERODYNAMICS)

Research performed at the D.E.R.A.T.

(October 1982 to September 1983)

STUDY OF THE PRINCIPLE RESULTS OBTAINED

Document Prepared for the Orientation Council Meeting

of 17 October 1983

Two primary activity areas:

A - FUNDAMENTAL STUDIES IN VISCOUS AND TURBULENT FLOWS

B - EXPERIMENTAL MEANS AND TESTING IN SUBSONIC-TRANSONIC FLOW.

1 - DEVELOPMENT OF MEASURING MEANS .....

1.1. - MEASUREMENTS OF SURFACE FRICTION USING HOT WIRE GAUGES (Tests at F1/CFM)

*4

Six gauges were installed within the upper surface of an LC 90 D airfoil, near the trailing edge. The flow is two-dimensional, velocity is constant and equal to 40 m/sec, the total pressure is equal to 1 bar and the angle of attack varies between -5 and +13 degrees. Boundary layer profiles were measured for each configuration and at different points using the hot wire anemometer technique. The form parameters measured in that manner were used in the Ludwieg- Tillman formula in order to obtain the changes in the friction coefficient against which the values obtained from the gauges are compared. This comparison reveals good agreement between the Cf changes obtained by the two methods; the relative differences are in the order of 10%, except in the neighborhood of the separation (indicated by an arrow) where the measurement technique is faulty.

1.2. - MEASUREMENT OF THE SURFACE FRICTION, THREE-WIRE GAUGE

To respond to the problem created by the measurement of the friction in unsteady boundary layers, various modifications were already added while building the wire gauges used in steady flow. These improvements make a large bandpass possible (much greater than 1000 Hz without an appreciable phase-shift) and also increase the sensitivity and the accuracy of the response of the probe in steady flow. The dispersion of the measurements performed does not exceed 3%

*Numbers in margin indicate foreign pagination

of the friction.

The determination of the sign of the friction can be obtained simply by adding two cold wires on each side of the sensitive element; these wires make it possible to locate the warm wake. The measurement principle is the following: the rod provides the friction coefficient and the two cold wires give the temperature upstream and downstream from the rod. The three signals being digitized, comparison of the temperature data against a threshold provides the sign of the friction.

The three-wire gauge has been used to determine the distribution of τ_p over a cylinder placed perpendicula y to the wind. Flow fluctuations induced by the release of Karman vortices are clearly revealed by the surface friction measurements: periodic displacement of the stagnation point and a sign change of the friction in phase ϕ = 180 degrees. On this last point, the instantaneous friction reaches rather large values, in the order of 3 to 5 Pa, whereas, for a reason of symmetry, the average value of τ_p must be equal to zero which is clearly shown by the signal processing that is performed.

1.3. - MULTIPLE PROBES

Hot-wire anemometer probes, multiwire probes (3 or 4 wire probes) have been used in order to define quickly and simultaneously the average and turbulent velocity fields of three-dimensional flows.

Adapting these new measurement techniques to the industrial environment has been attempted in the F1 wind tunnel of Le Fauga during tests to define vortex areas close to a sweptback

wing. Some difficulties inherent to the geometry of the probe itself and to the highly vortex-filled nature of the flow (rate of turbulence close to 50%) have appeared and have led to the increase of the stiffness and strength of the sensor. On the other hand, a new method for calibration and operation has been considered so as to push back the limitations in the use of the probe in turbulent flows that have been highly deflected.

Legend:

1 - Thermocouple

2 - Stainless steel

3 - Tungsten wire - Diameter 5 µm

4 - Balsa disk

5 - Polyester resin

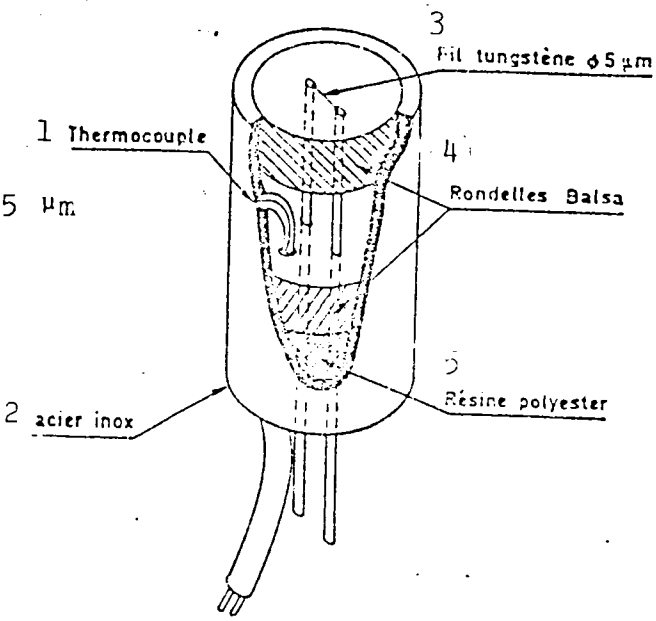

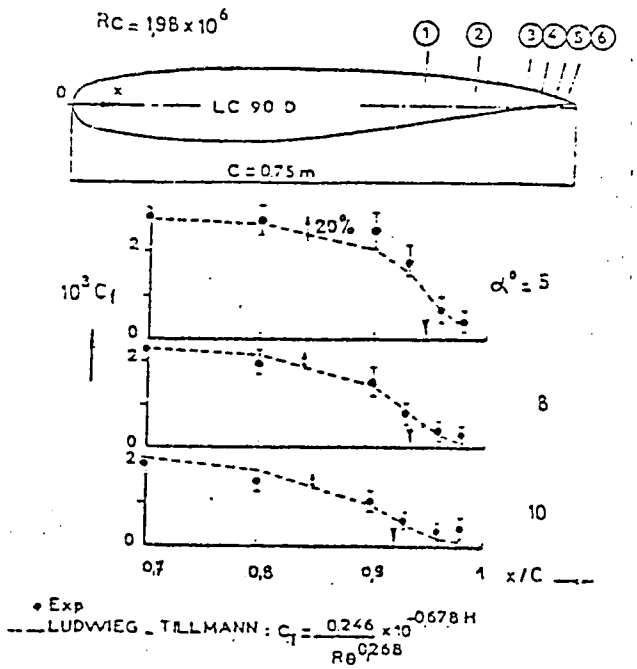

FRICTION OVER LC90D AIRFOIL AT F1

Legend:

1 - Upstream cold wire

2 - Hot sensitive element

- Diameter: 75 µm

3 - Downstream cold wire

4 - Cross-section plane

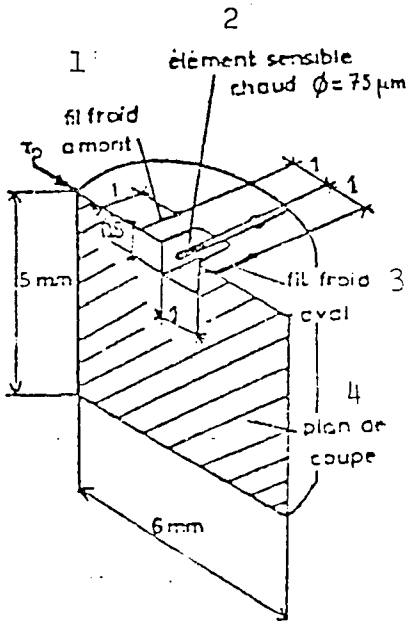

THREE-ELEMENT GAUGE

Legend:

1 - Sign of the velocity

2 - Coarse signal

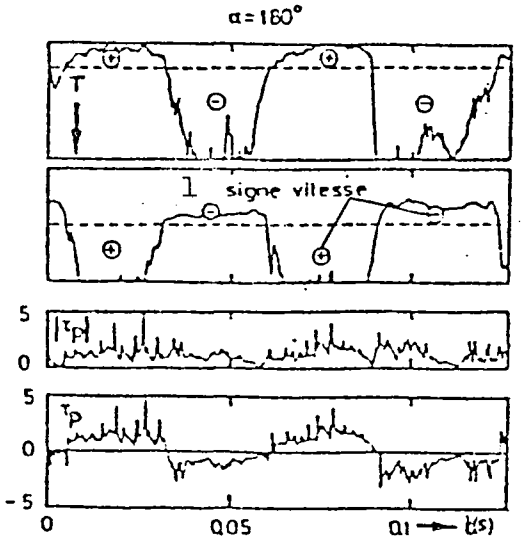

SIGNAL PROCESSING

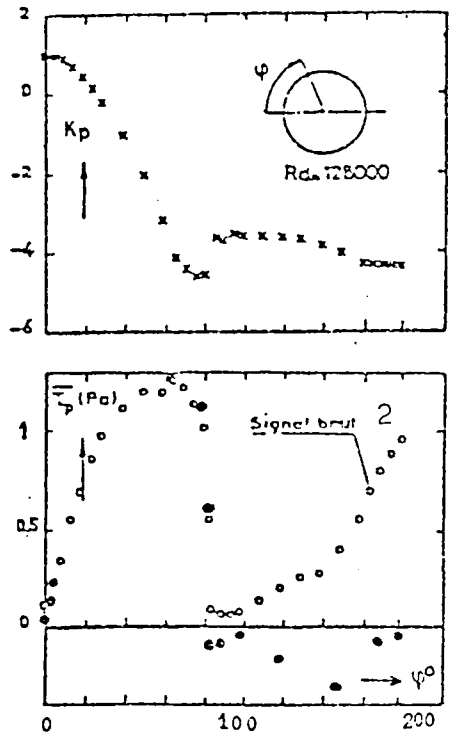

FRICTION OVER CYLINDER

2 - PREPARATION OF TESTS AT WIND TUNNEL F2 AT LE FAUGA

This wind tunnel, used by GME, is designed for the basic research work of the ONERA and DERAT Directorate of Aerodynamics: complex three-dimensional configurations, the process of turbulence generation, the check of computation methods. 6

The primary characteristics of the wind tunnel are:

- atmospheric pressure,
- velocity: 0 to 100 m/s
- test section:
  - width: 1.40 m
  - height: 1.80 m
  - length: 5 m
- cross-section reduction ratio 12, low amount of turbulence.

The side walls of the test section are easily removed. They are opaque or transparent depending on the need. The movable support of the laser velocity-measuring device that surrounds the test section provides a longitudinal displacement of 3.75 meters, a vertical displacement of 1 meter and a transverse displacement of 0.6 meter from the aiming point, thus defining a large volume for test purposes.

The first experiments will be performed by the DERAT and will have as parallel goals the refinement of existing measuring systems (LDA in particular) and the definition of other means of measurement (hot wire exploration, for example).

The assembly used will be a cylinder with a diameter of 12 cm, motor-driven in rotation about its axis. It will make

it possible to conduct a fine and detailed study of the flow about the cylinder (average and fluctuating pressure, surface friction) with an accuracy of 0.1 degree by using a single generatrix of the cylinder. In particular, we will be interested in the area near the separation point and the stagnation point. Visualizations using a laser plane are also planned.

A second thrust of the studies will be the cylinder wake. The size of the test section will indeed make it possible to explore the distant wake (up to 40 diameters) and the characteristics of the wind tunnel will make it possible to conduct tests up to Renolds numbers of 700,000, that is to say beyond the critical Reynolds number.

There again, visualizations using a laser plane are planned.

3 - UNSTEADY BOUNDARY LAYERS - COMPUTATION USING SMALL PERTURBATIONS

For the computation of the incompressible two-dimensional unsteady flow boundary layers, a method using small perturbations can prove very interesting by the rapidity with which it can be applied in all cases where the boundary conditions of the problem are periodic. The success of this type of method rests primarily on the fact that the non-linear effects are small, as has been shown experimentally or through integration of the complete boundary layer equations. 8

The application of such a method in the more general case of a compressible three-dimensional boundary layer was necessary for certain practical applications of interest to industrialists such as the prediction of buffeting or flutter.

Principle of the method

To the three force, longitudinal momentum and transverse momentum integral equations, there are three primary unknowns H, θ_{11}, θ_{21} which are the form parameters and the thicknesses of longitudinal and transverse momentum respectively.

The system may be put in the form:

$$\sum_{j=1}^{3} \left(Ex_{ij} \frac{\partial y_j}{h_1 \partial x} + Et_{ij} \frac{\partial y_j}{u_e \partial t} \right) = E_{si}$$

$i = 1, 2, 3$ designates the equation considered and y_j, $j = 1, 2, 3$ represents the major unknowns. h_1 is the length component in the x direction making an angle α with the outside velocity. The E coefficients are implicit functions

of u_e, α, $\frac{\partial \alpha}{h_1 \partial x}$, θ_{11}, H, θ_{21} by means of a set of closing relationships, and of the derivatives of u_e in the z direction, making an angle λ with respect to x.

The small perturbation hypothesis consists of assuming that any f value can be written in the form:

$f = \bar{f} + f_c e^{i\omega t} + f_{cc_e} -i\omega t$ with f_c the complex amplitude and $\frac{f_c}{f} << 1$.

The system of equations then transforms itself into two systems of three equations, one for the average values of the unknowns and not revealing fluctuating quantities, and the other for the complex amplitudes of the unknowns and a function of the average values. If the integration of the average system does not create a problem (it is identical to the system for the steady-flow problem), the integration of the unsteady system requires the computation of the complex portion of the E coefficients. The latter being a function of the independent variables, we have: $E_c = \sum_i \frac{\partial E}{\partial i} x_{ic}$, where x_{ic} represents the complex amplitude of x_i. The computation of the partial derivatives of E relative to the x_i's can be done algebraically in part or in a purely numerical manner by computing i values of E for increases of the xi's. The two procedures provide identical results but the second is faster in terms of machine time. Practically, the small-perturbation method requires only three times the amount of time for the steady-flow method. For one node in the mesh, 0.053 second is required.

In 2-D or 3-D incompressible flow the non-linearity effects remain very low and the method applies for $\Delta Ue/Ue \leq 0.20$.

In incompressible flow (Me $\simeq$ 1.6), these effects become appreciable as soon as $\Delta Ue/Ue$ reaches several percentage points.

Legend:

1 - Assembly area

2 - Control room

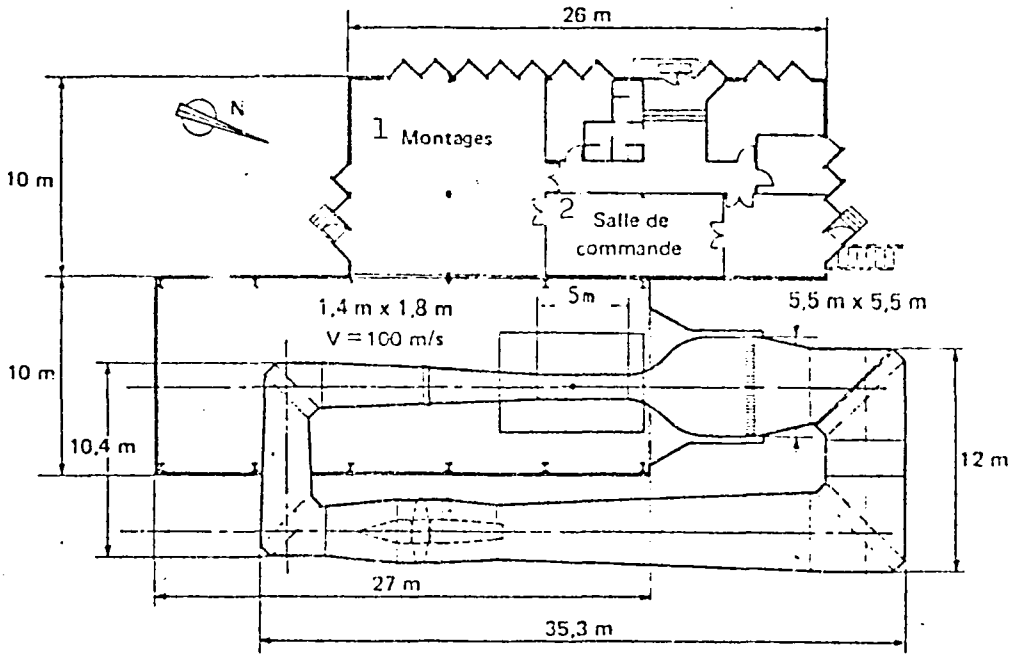

Aerodynamic circuit and technical rooms.

- Test section and movable support for the velocity-meter

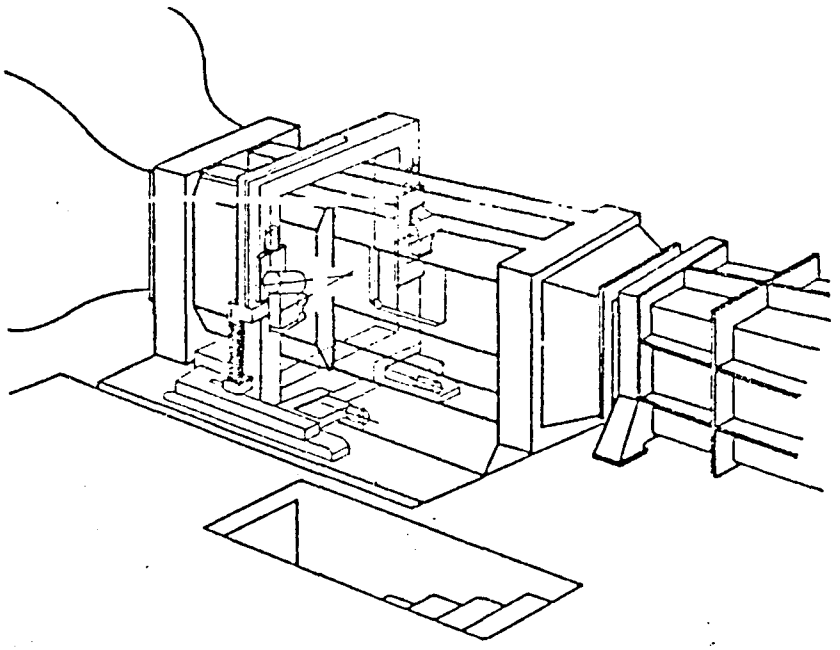

Legend:

3 - Motor drive

4 - Pressure intakes

5 - Cf gauges

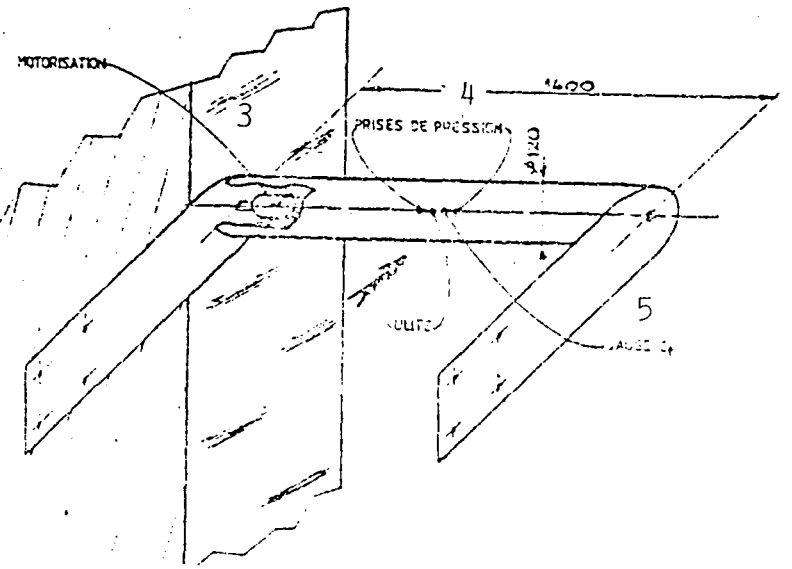

- Set-up of a circular cylinder facing into the wind

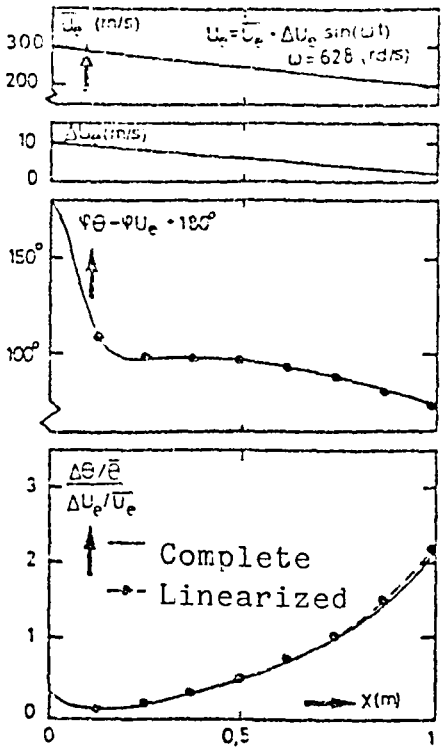

Two-dimensional Boundary Layer Momentum

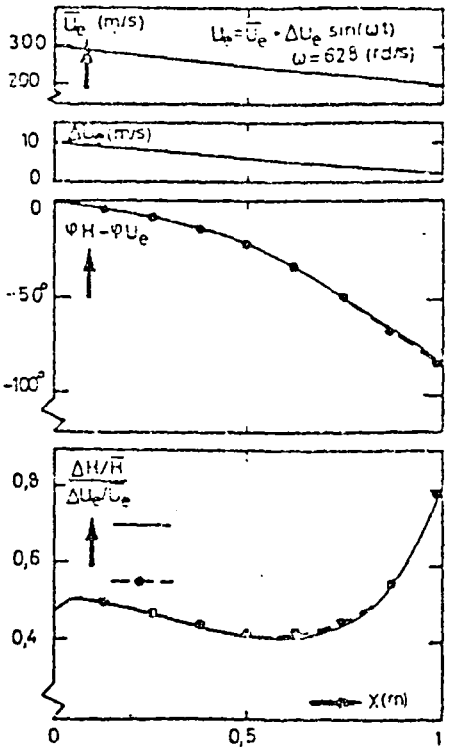

Two-dimensional Boundary Layer Form parameter

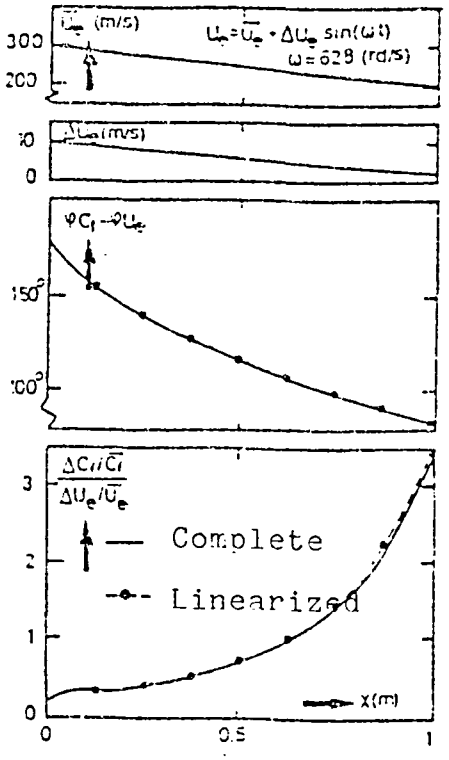

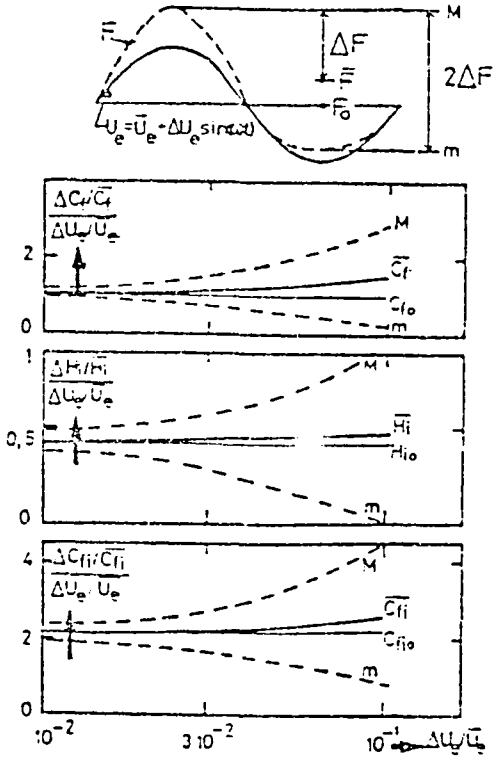

Two-dimensional boundary layer

Surface friction

Pie = 1.2×10^5 Tie = 294 K

$\bar{\theta}_o = 10^{-4}$ m $\quad \bar{H} = 1.9$

Non-linearity effects due to compressibility

$\bar{U}_e$ = 500 m/s Pie = 1.2×10^5 Pa

Tie= 298 K - Two-dimensional Boundary layer

$\theta_{11_o} = 10^{-4}$ m $\quad \left(\frac{\Delta H/H}{\Delta U_e/U_e}\right) = 1.56$

4 - BOUNDARY LAYERS OF BODIES OF REVOLUTION AND OF FUSELAGES

4.1. - COMPUTATION OF OUTSIDE STREAMLINES

The computation of the three-dimensional boundary layer requires that conditions be given at the limits, that is to say the magnitude and direction of the velocity of the non-viscous flow. 10

If the latter is determined from a perfect fluid computation, the velocity is simply broken down along the axes of the reference frame in which the boundary layer is computed.

On the other hand, if the non-viscous flow is only known from the distribution of the surface pressures, it is necessary to compute the direction of the velocity. The latter is determined in two steps. The streamline passing through a given point is first computed in reverse: the direction of the velocity at that point is adjusted through an a firing method so that the streamline ends at the stagnation point. This direction is then used to complete the solution downstream.

This procedure has been applied to Airbus-type fuselages around which the pressure distribution has been obtained by means of a perfect fluid computation. The comparison of the directions of the velocity is entirely satisfactory.

4.2. - BOUNDARY LAYER COMPUTATION

The program for the three-dimensional boundary layer that was developed at the DERAT has been adapted to the case of fuselages (problems associated with the periodicity of the geometry and to the definition of transverse data at the ends

of the z grid).

The program has been used for the computation of the boundary layer that develops over the nose of the Airbus-type aircraft. The separation at the bottom of the windshield is characterized by a large deflection of streamlines along the wall with respect to outside streamlines.

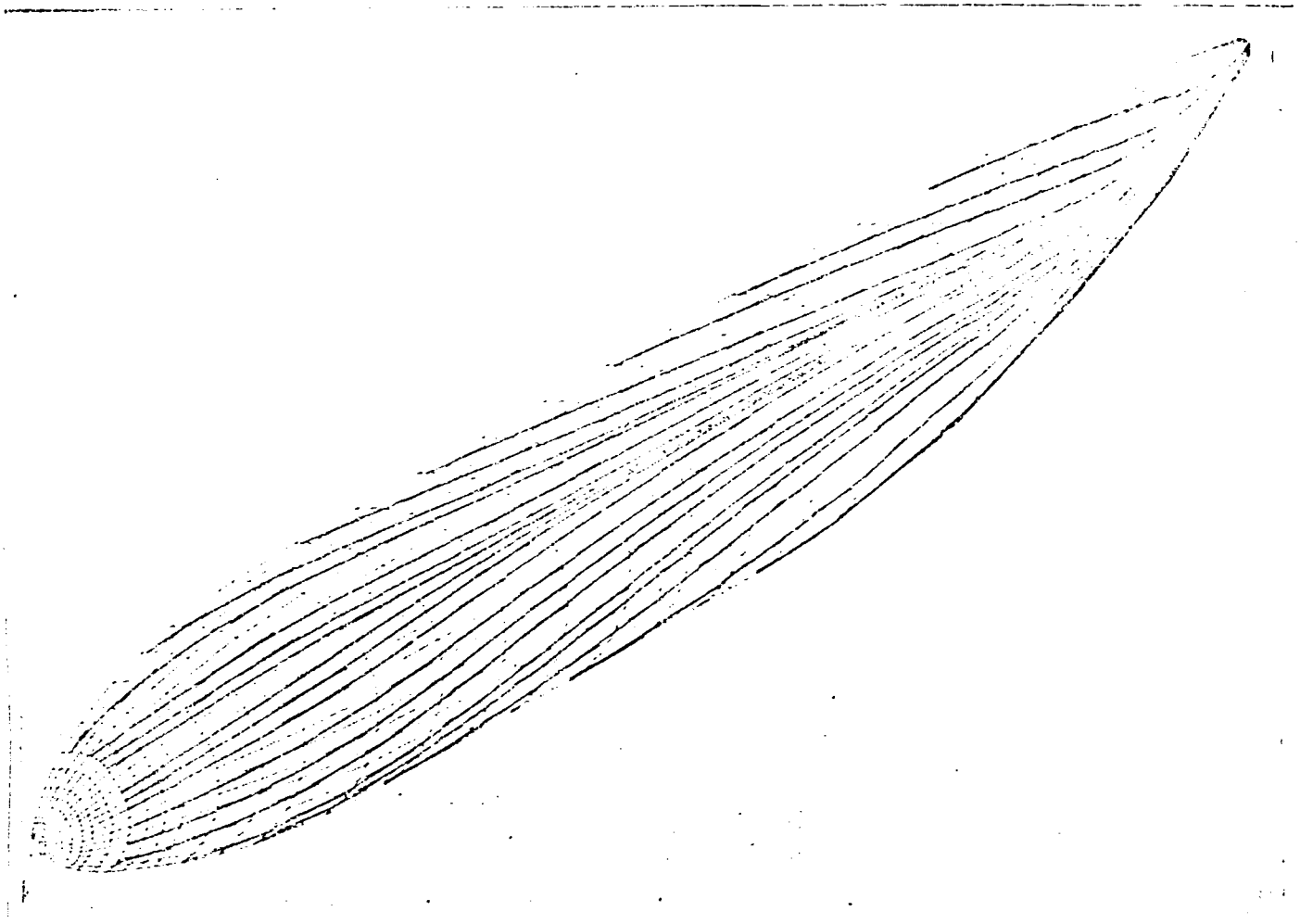

FUSELAGE - M_∞= 0.8, angle of attack: 5 deg, slip angle 4 deg.

Plot of outside streamlines.

Nose

$M_\infty = 0.8$

angle of attack: 0 deg

slip angle : 0 deg

Plot of streamlines:

- outside streamlines are shown in black
- surface streamlines are shown in red.

  They appear as the solid lines on this reproduction.

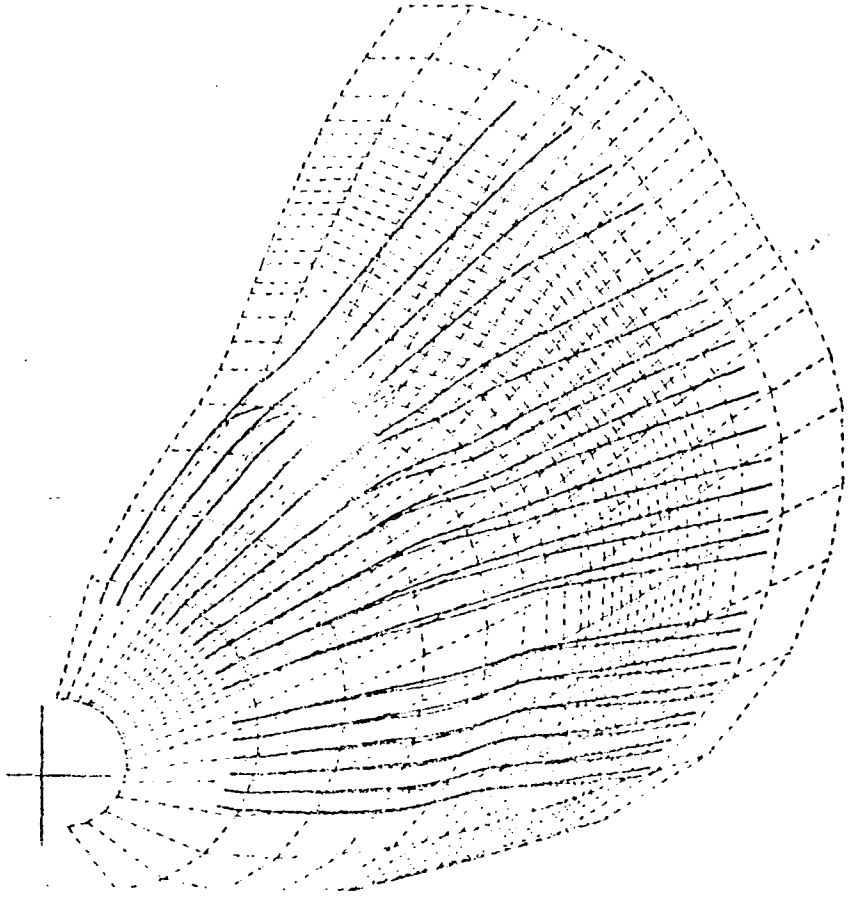

5 - PROBLEMS ASSOCIATED WITH WING-FUSELAGE INTERACTIONS

5.1. - NUMERICAL STUDY

The case of the Shabaka experiments was treated in detail in order to study the performances of the various turbulence models. A symmetrical wing without sweep or angle of attack is placed on the floor of the wind tunnel. The computation begins 19 cm downstream from the leading edge of the wing, using the initial experimental data which indicate the presence of a strong vortex. The equations are made parabolic in the direction of the primary flow. The main problem consists of modelling the Reynolds stresses:

Vortex viscosity model

This is the simplest of all. The $\overline{u'_i u'_j}$'s are of the form: $$\overline{u'_i u'_j} = \frac{2}{3}\delta_{ij} - \nu_t \left(\frac{\partial Ui}{\partial xj} + \frac{\partial Uj}{\partial xi}\right)$$

k represents the turbulence kinetic energy and ν_t is the turbulent viscosity obtained, by example, through a formula for the length of the mixing. This model gives good results.

"Complete" transport equations for the Reynolds stresses

It is the most advanced model since it solves six equations for the six components of the Reynolds tensor:

$$\frac{\overline{Du'_i u'_j}}{Dt} = Pij + Dij + \phi ij + \frac{\partial Jijk}{\partial x_k}$$

This model is defined as "complete" in the sense that all of the derivatives of the three components of the average speed are retained. The Launder-Reece-Rodi modelling is adopted for the redistribution term Øij. The solution of

a transport equation for the dissipation makes it possible to close the system. The results obtained resemble those given by the vortex viscosity with, however, a certain displacement of the center of the vortex.

System (6.6)

In the preceding model, we neglect the convection and diffusion terms but we keep all of the $\frac{\partial Ui}{\partial xj}$'s. At each computation node, it is necessary to solve a linear system of six equations for the six stresses. With respect to the results, there are few differences from the solution of the complete equations.

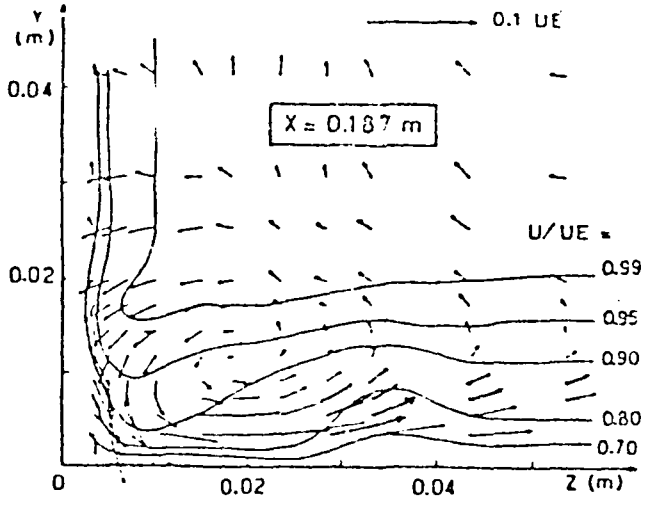

Initial data

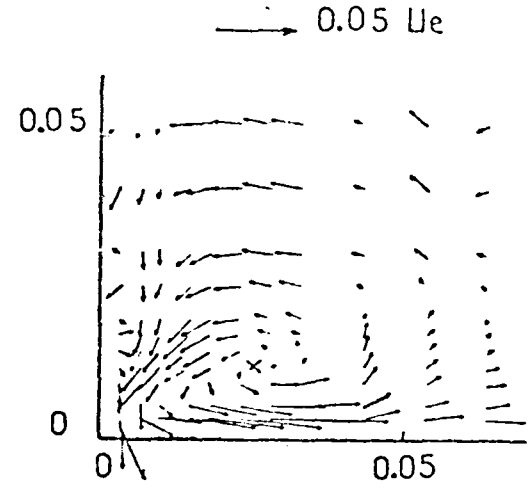

X = 1.25 m

EXPERIMENTAL RESULTS (SHABAKA)

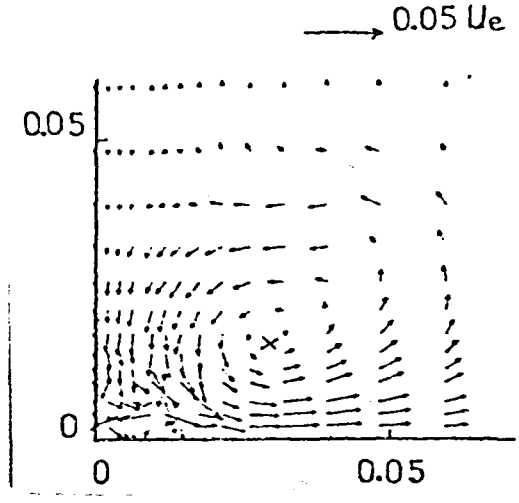

Vortex Viscosity

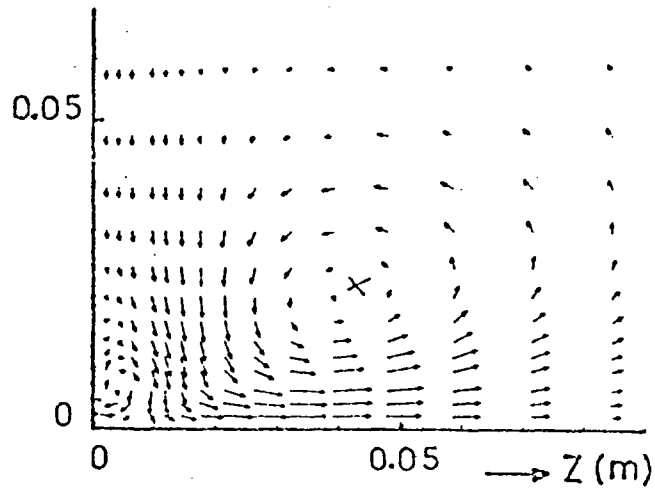

Six Transport Equations

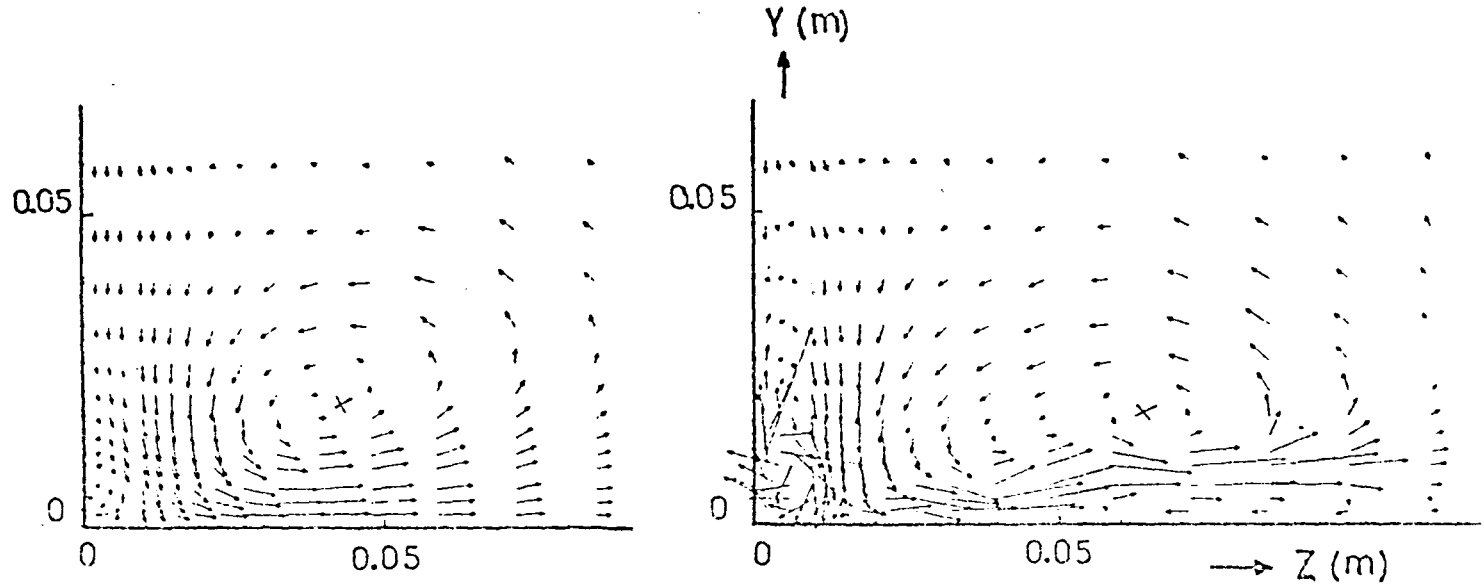

System (6.6) Algebraic model

COMPUTATION RESULTS (X = 1.25 meters)

Algebraic model

In the preceding system only the derivatives $\frac{\partial U}{\partial y}$ and $\frac{\partial U}{\partial z}$ are

retained. The Reynolds stresses are then expressed by means of simple analytical formulas, but the computation is in poor agreement with the experiments.

Thus it appears that the derivatives of the secondary velocities V and W play important functions in the modelling of the $\overline{u'i\ u'j}$'s. The vortex viscosity model, combining accuracy and a small number of computations, seems to be the most interesting but it cannot compute the development of the vortices created by turbulence. The model with six "complete" equations (or the system (6.6) in cases that are slightly convective), although more awkward to handle, offers, on the other hand, a greater range of applications.

5.2. - STUDY OF THE MIXING OF A FUSELAGE BOUNDARY LAYER AND OF THE WAKE FROM A WING

The experimental setup consists of an ONERA D wing airfoil with a chord length of 200 mm placed perpendicularly on the floor of the test section. Sweep and incidence angles are equal to zero. 14

The goal of the study is to study the three-dimensional mixture of the boundary layer on the floor which simulates a fuselage and of the wake generated by the wing.

A first set of experiments had the purpose of defining the conditions away from the floor, that is to say the development of the boundary layer and of airfoil wake. The velocity measurements have been accomplished over a rather tight grid with the help of a hot wire anemometer. The static pressure profiles were also measured.

Then, measurements of the wake-boundary layer mixture were performed with the help of a probe with five pressure tubes. The mapping of the secondary velocities and the lines of equal velocity were thus defined. They show in particular the rapid change in the nature of the flow near the trailing edge. In particular, the junction of the trailing edge and of the floor behaves as a hole for the secondary velocities.

5.3. - EXPERIMENTAL STUDY OF THE FLOW IN THE NEIGHBORHOOD OF THE CONNECTION BETWEEN A FUSELAGE AND A SWEPTBACK WING WITH AN ANGLE OF ATTACK

The experimental study consists of a wing airfoil (ONERA D airfoil with a chord length of 200 mm) placed with a large

sweep angle (60 deg.) and at an angle of attack (15 deg.)

A measurement of the field of average velocities was performed with the help of a five-hole level indicator probe set within the angle defined by the wing and the floor of the test section. Nine planes were measured at X = -50 mm, 50 mm, 100 mm, 150 mm, 200 mm, 250 mm, 300 mm, 350 mm, 382 mm (X is measured from the leading edge).

Measurements made with the help of a hot wire anemometer probe (probe with one straight wire) were undertaken in order to validate the results obtained by the five-hole level indicator probe (with regard to the magnitude of only the velocity vector) and also to define the u'^2 component of the Reynolds tensor before undertaking a complete definition (6 components of the Reynolds tensor) of the turbulent field with the help of a four-hot wire anemometer probe.

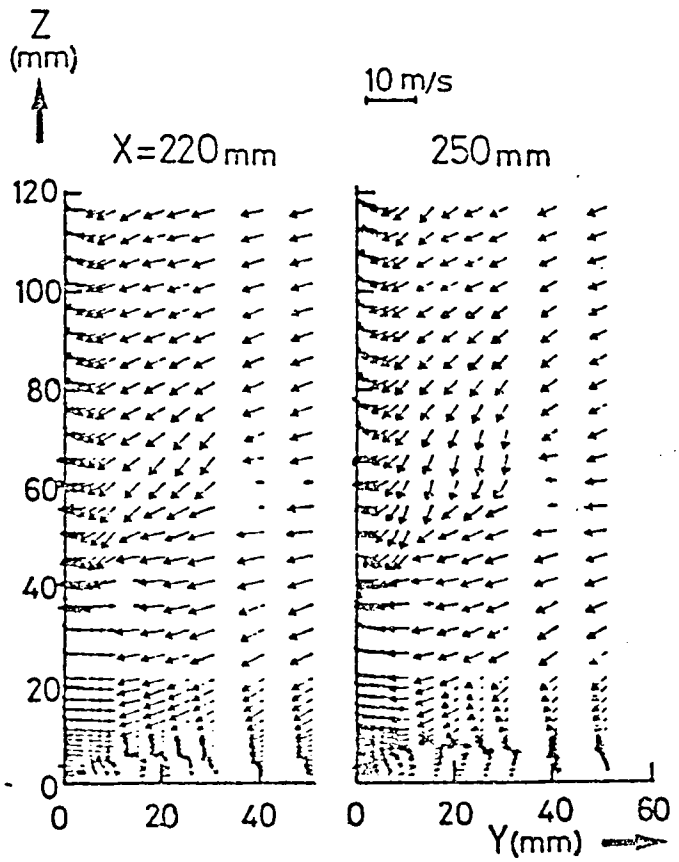

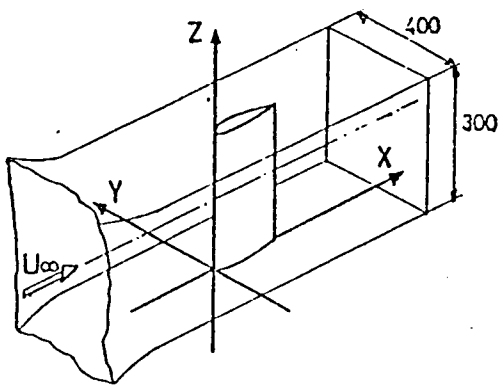

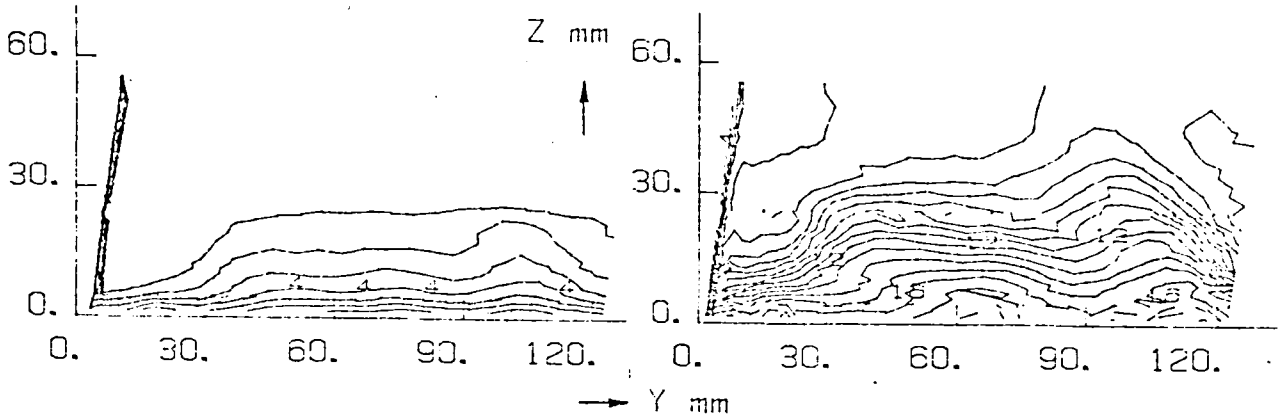

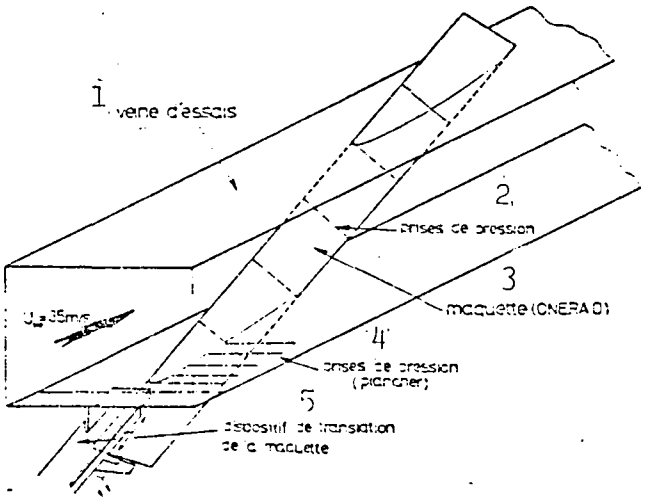

15

Legend:

1- Test section

2- Pressure taps

3- Model (ONERA-D)

4- Pressure taps (floor)

5- Device to translate the model

6 - MODELLING TURBULENCE

6.1. - EFFECTS OF ROTATION ON TURBULENCE

A general rotation of the flow, applied to an homogeneous and initially isotropic turbulent field, lessens the rate of decrease of the turbulent energy. However, this effect was not taken into consideration in the standard turbulence models. 16

It had already been demonstrated that a simple modification of the EDQNM two-point closing model makes it possible to show the effect of rotation on spectral energy transfers. This EDQNM model has been validated at very low Reynolds numbers by comparison with direct simulations of Navier-Stokes equations and at a moderate Reynolds number by comparison with simulations of large structures. In this latter case, the sub-node model describing the effect of small scales on large structures is derived from the EDQNM model.

The next step consisted of performing a large number of numerical simulations of turbulence in rotation for a broad range of energy spectra, of Reynolds numbers, and of rotation rates with the EDQNM model. The trend analysis of the dissipation rate of the kinetic energy ε as a function of time has provided a new model of the transport equation for this dissipation rate. Comparison with an experiment, in this case the experiment of Wigeland and Nagib, has made it possible to check the validity of the model.

One significant point of the study of the rotation is that the shear encountered, inside the boundary layers for example, breaks down into a planar deformation and a rotation. Taking

the effects of rotation into consideration in the transport equations models of turbulent stresses has led to the improvement in predicting, both with cases of low shear and of high shear.

6.2. - SPECTRAL INTEGRAL METHOD

The spectral integral method is a new approach to formulating transport equations for turbulent quantities. It relies on a hypothesis defining the form of the sprectrum of the kinetic energy of turbulence. For the time being, this model is only used to improve the prediction of the dissipation rates of the kinetic energy ε.

In the case of a mono-scale model, the spectral integral model gives a new transport equation for ε without an adjustable constant, contrary to the standard model. The trend of the dissipation rate is then tied to the production/dissipation balance and to the evolution of the very large structures that can be computed directly with a linear model. The prediction of the cases of homogeneous turbulence subjected to a flow is further improved.

In the case of a multi-scale model, the energy spectrum is split into two areas: one describes the large structures carrying energy, the other describing the small structures of the inertial and dissipative areas. The spectral integral method makes it possible to replace the two transfer equations for the energy flow from the large structures toward the small structures and for the dissipation rate with one simple hypothesis in the form of the spectrum and one equation for

the energy flux directly derived from the sub-node models developed at the DERAT. The multi-scale model is sensitive to the division of the production term between large and small structures. In the cases of pure rotation (no production), it gives very good results. Results close to and even better than those obtained with the mono-scale model are given with very intuitive divisions of production.

TURBULENCE HOMOGENEOUS IN ROTATION

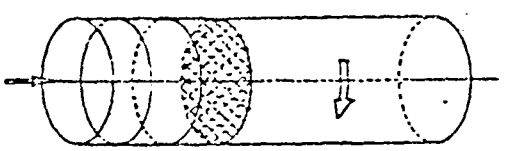

Honeycomb Grid Test section in rotation

Corrections of the equation for ε

$$\omega^* = \frac{\omega\, l/2q^2}{\varepsilon}$$

o computation without correction

A proposed model

B Bardina model

HL Hanjalic and Launder model

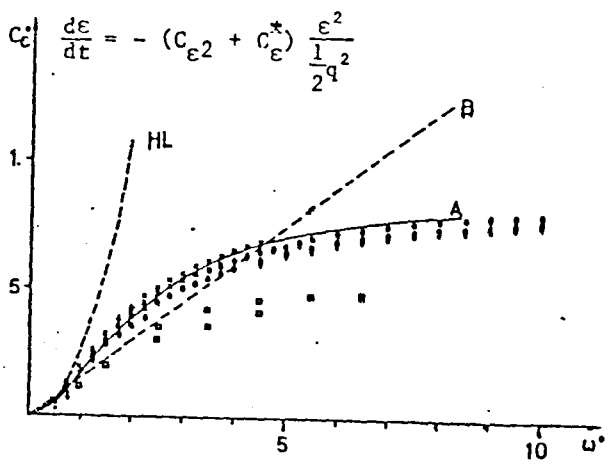

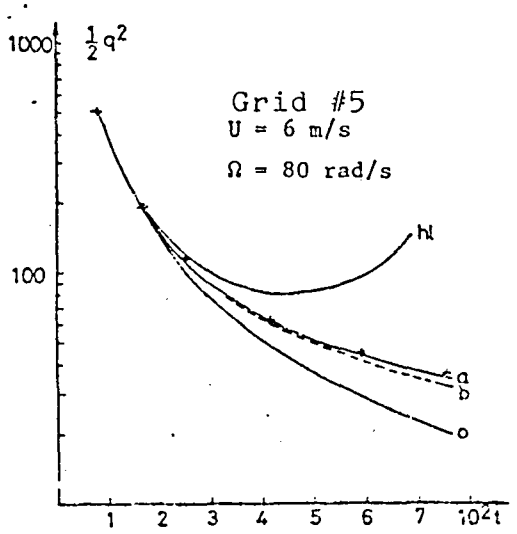

HOMOGENEOUS TURBULENCE SUBJECTED TO A SHEAR

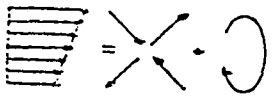

Shear = deformation + rotation

Champagne experiment

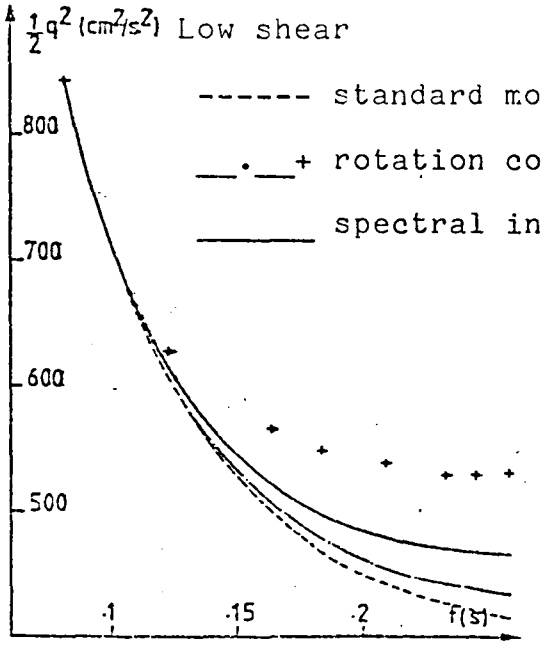

Harris Experiment

High shear

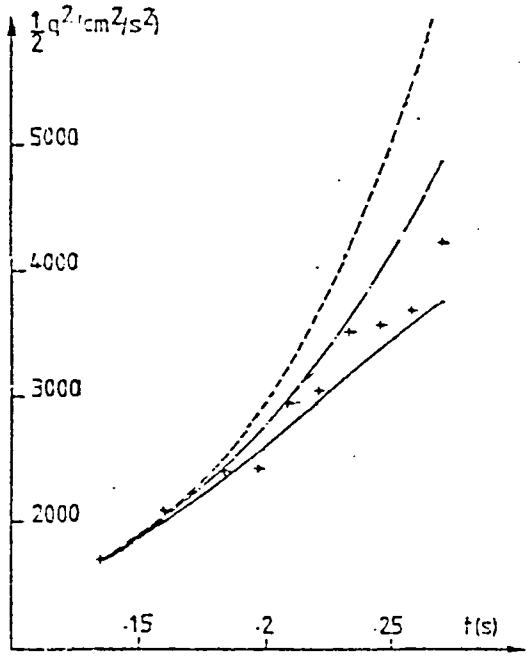

7 - DEVELOPMENT OF COMPUTATION METHODS

7.1. - SOLUTION OF THE NAVIER-STOKES EQUATIONS PARABOLIZED IN THE TWO-DIMENSIONAL WITH SIMULTANEOUS COMPUTATION OF p, u, v.

18

The Navier-Stokes equations are solved for two-dimensional laminar flow problems by means of a method called semi-elliptical. We take into account transverse variations of the longitudinal pressure gradient but the diffusion terms in the primary direction of the pressure gradient are neglected. In addition, the longitudinal component of the pressure gradient is approached through a formula that is decentralized so as to recover the elliptical effects due to the pressure.

The numerical method used is intended to solve the system formed by the equations of motion and the continuity equation so that the velocity and pressure fields are computed simultaneously. The simultaneous handling of the equations indeed assumes a primordial significance in obtaining fast convergence and makes it possible to overcome difficulties such as separation at the trailing edge of an airfoil. Strong coupling between the viscous and non-viscous areas of the flow is automatically obtained. The system to resolve is written in the matrix form AX = B where X is a column vector having as components all of the variables of the system at the point where it is computed. Matrix A is a matrix that is tri-diagonal in blocks that we seek to inverse. The problem is solved step by step following the increasing values along the abscissa but the presence of the pressure terms

downstream from the computation abscissa implies the iteration of the process until convergence is obtained. This method requires only the storage of the pressure at all nodes in the mesh, the determination of U and V at the point where the computation is made implying the knowledge of these variables only at the previous point of measurement. This consideration together with the fact that convergence takes place rapidly provides this technique with a definite advantage in comparison with other methods that are classically used to solve this type of problem.

The procedure described below has been checked for two different problems:

The first of these studies refers to the flow around the trailing edge of a flat plate. The results of the semi-elliptical method are in excellent agreement with those obtained by classical coupling methods and with those obtained by the solution of the complete Navier-Stokes equations.

The flow around a descending step is the object of the second application. Here, the longitudinal diffusion terms have been retained in the neighborhood of the step, downstream from it. The results are close to those obtained by more refined methods of the Navier-Stokes equations but the computation times are much less.

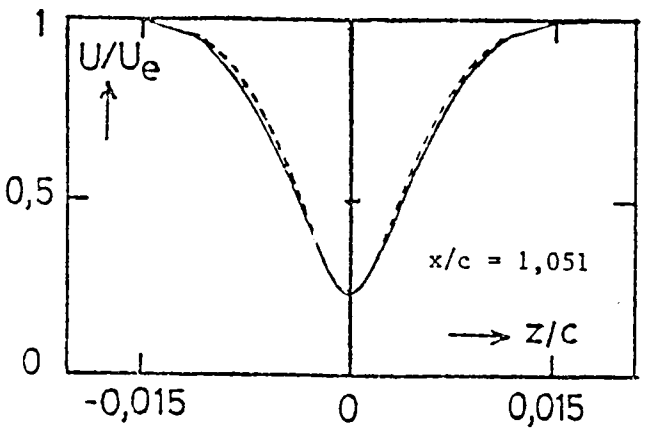

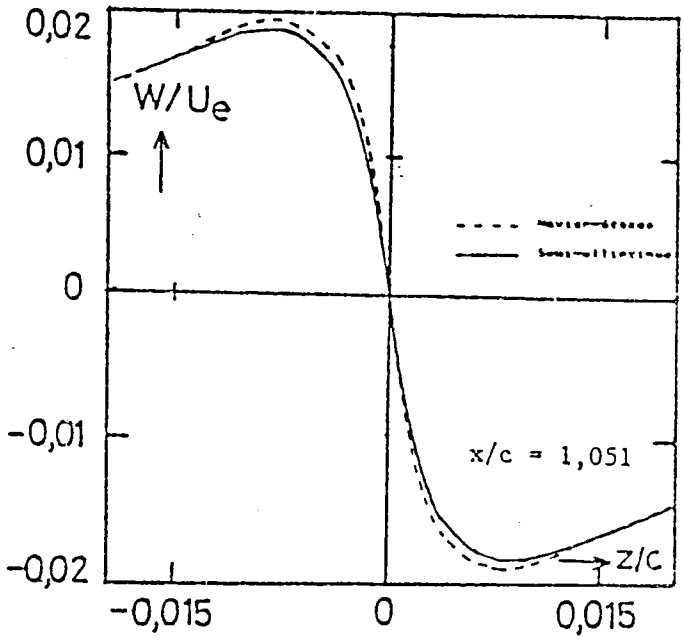

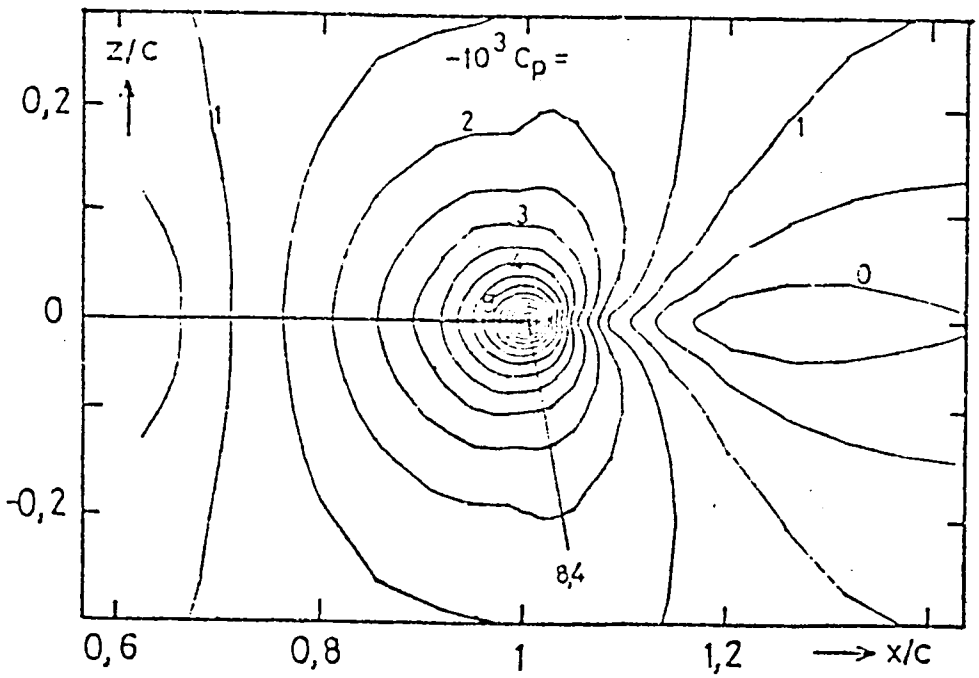

Flat Plate

$R_c = 10^5$

Flat plate - isobar lines - semi-elliptical method

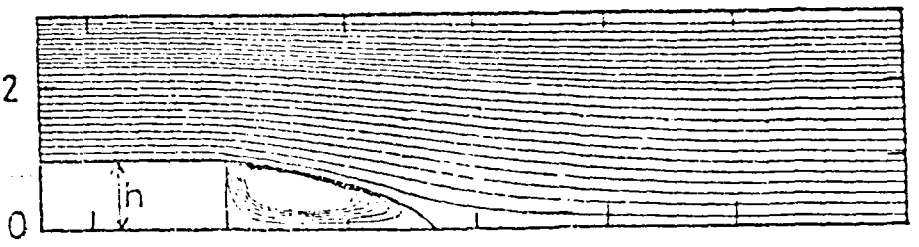

Channel with a step - semi-elliptical method Rh = 50 Streamlines

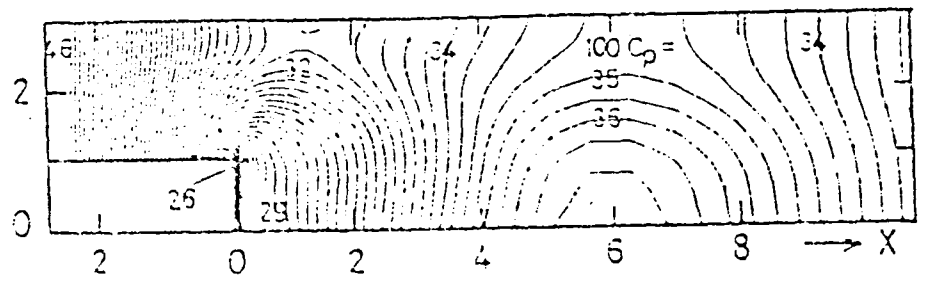

Isobar lines

7.2. - BOUNDARY LAYER-PERFECT FLUID SIMULTANEOUS COMPUTATION WITH INTERACTION. APPLICATION TO SEPARATION BULBS.

20

For the computation of the flow about an airfoil, it is often advantageous to separate the viscous effects from the non-viscous effects. The area close to the airfoil will be governed by the boundary layer equations, the rest of the area being governed by the perfect fluid equations, Then,we will have to take into account an interaction between these two areas.

An attractive solution method consists of solving the two problems simultaneously (Veldmann). Formally, the problem appears in the form:

$$\delta_1 - CL\ (Ue) = 0 \quad \text{and} \quad \delta_1 - FP\ (Ue) = 0$$

where CL and FP represent the boundary layer and perfect fluid operations linking the flow velocity Ue and the displacement

thickness δ_1. Let us note that because of the elliptical nature of the non-viscous problem, an iterative process must be applied.

This method has been applied to the computation of separation bulbs with transition for which a method of the inverse type has been developed.

The boundary layer is computed with the help of an integral method for the laminar, turbulent or transitional regimes. The perfect fluid is considered as the result of the superposition of a known non-perturbed state and of a correction which is determined by computing a Cauchy integral. In that manner, the coupling problem involves only one space variable.

The boundary and perfect fluid equations as well as the interaction rule connecting them are solved simultaneously by means of a relaxation method.

The results have been compared against those obtained with the standard inverse method: they are very close to those results but provide a very considerable reduction in computation time.

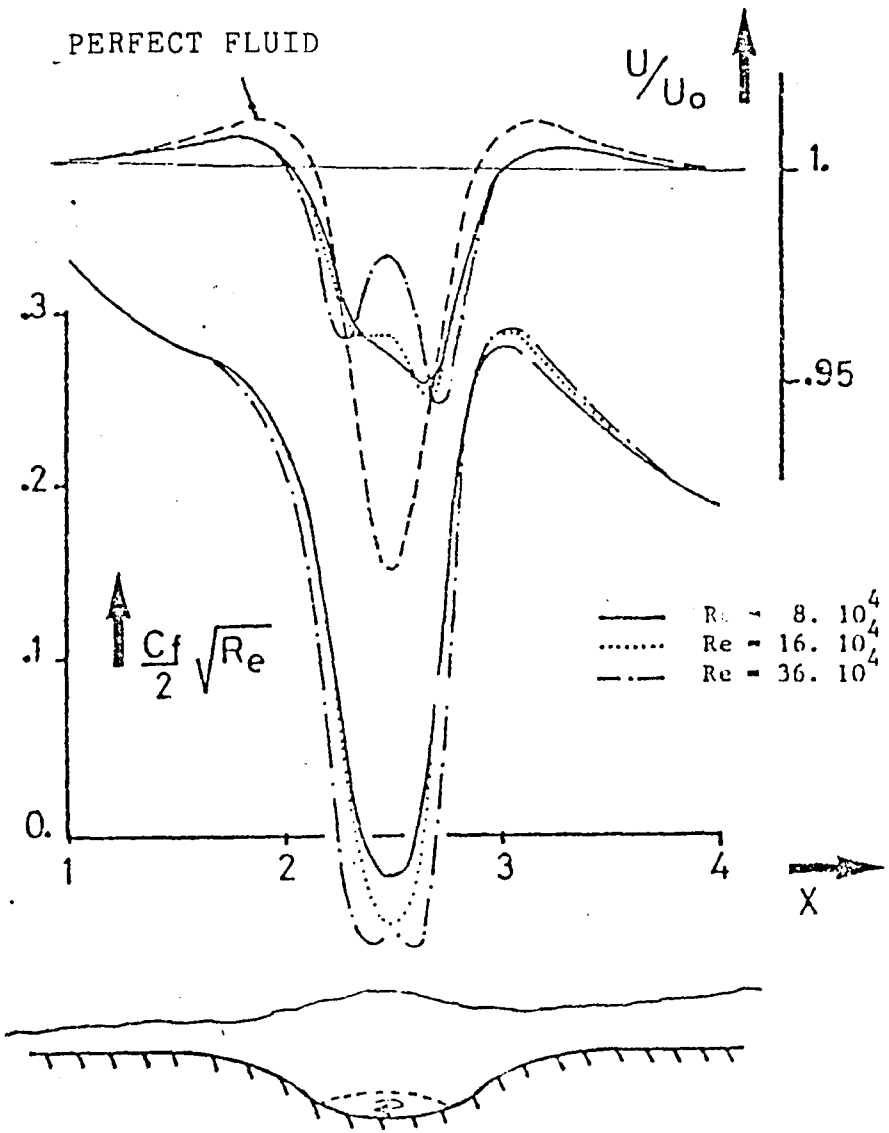
PERFECT FLUID
U/Uo
1.
.95
.3
.2
.1
0.
Cf/2 √Re
Re = 8. 10^4
Re = 16. 10^4
Re = 36. 10^4
1
2
3
4
X

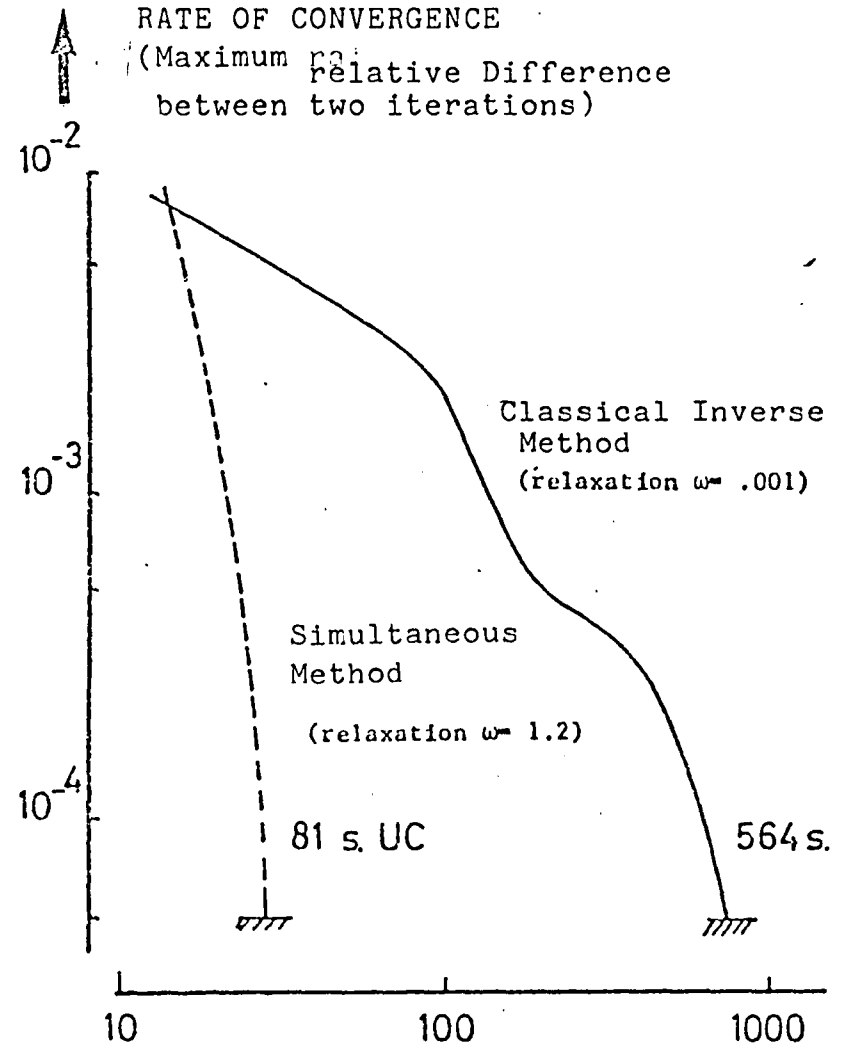
RATE OF CONVERGENCE
(Maximum relative Difference between two iterations)
10^-2
10^-3
10^-4
Classical Inverse Method
(relaxation ω= .001)
Simultaneous Method
(relaxation ω= 1.2)
81 s. UC
564 s.
10
100
1000
NUMBER OF ITERATIONS

8 - TRANSITION OF THE BOUNDARY LAYER IN THREE-DIMENSIONAL FLOW

8.1. TRANSITION CRITERIA AND STABILITY

In the absence of contamination of the leading edge laminar boundary layer by the turbulent boundary layer of the fuselage, the existence of the transition, on a sweptback wing, is due to two types of instabilities: longitudinal instability and transverse instability which appears, when it exists, much closer to the leading edge. 22

For the first type of instability, a two-dimensional criterion (or "longitudinal") is applied along an outside streamline.

For the transverse instability, two criteria have been developed:

. one entirely empirical formula binds a Reynolds number of the transverse velocity profile to the form parameter of the longitudinal profile:

$$R\delta_2 = \frac{1}{\nu} \int_0^\delta W_1 \, dy = f(H_1)$$

. one more refined criterion uses the results deduced from the theory of laminar instability. For a Reynolds number with a fixed chord and abscissa value, the stability properties of the velocity profiles U_ε projected in a direction ε are studied from $\varepsilon = 0^\circ$ (direction of transverse flow) to $\varepsilon = 90^\circ$ (direction of the longitudinal flow).

The evolution of the function $g(\varepsilon)$ - ratio of the critical Reynolds number $\mathcal{R}_{\delta_1}{}_\varepsilon$ of the U_ε airfoil to the Reynolds number $\mathcal{R}_{\delta_1|\varepsilon}$ of this same airfoil is obtained at various abscissa values. The values that make the function g a minimum correspond to the most unstable directions. In the range

of low values of ε ($0 < \varepsilon < 10^\circ$), the most unstable direction ε_{min} is responsible for the transversal instability, or rather quasi-transverse since it differs from the transverse direction by several degrees. The transition criterion is then obtained by an empirical correlation between, on the one hand, the Reynolds number formed with the displacement thickness of the velocity streamline projected in the direction ε_{min} and, on the other hand, the form factor of the longitudinal airfoil H_1 and the rate of outside turbulence: $R\delta_{1\varepsilon(\varepsilon=\varepsilon_{min})} = g\ H_1(Tu)$. The application of these criteria in various series of experiments, including that of Boltz-Kenyon and Allen, has given satisfactory results.

8.2. - COMPUTATION OF THE TRANSITION REGION

The abscissa of the beginning of the transition being known, it is now necessary to compute the transition region itself. A standard method, known under the name of intermittence method, is used. A model relying on an equilibrium of the laminar and turbulent properties of the boundary layer has first been established by computing two-dimensional boundary layers through solution of local equations. It was then extended to the three-dimensional case. In addition, a first approach to a model for the solution of the integral equations of the boundary layer in the two and three-dimensional has been studied; it is already providing encouraging results.

8.3. - PARAMETRIC STUDY OF THE SWEEP ANGLE EFFECT

The OAP 01 airfoil (glider wing airfoil) is studied at three

angles of attack: 0°, 1° and 2°. On the upper surface, the distributions of the outside velocity are of the "laminar" type, with steep negative pressure gradients. There results from it a large transverse flow, and providing a sweep angle brings the transition closer to the leading edge. On the other hand, on the lower surface, the distributions are "flatter". The transverse flow, much weaker, has little chances to lead to a premature transition. Nevertheless, this transition exists but it is due to a longitudinal instability. The complete computation of the laminar, transitional and turbulent regions provides the variations of the thickness of the momentum at the trailing edge, θ_{BF}, which makes it possible to estimate the total drag coefficient.

Parameter measuring is performed as a function of the angles of attack and of sweep. In that manner, we show the effect of the sweep angle at a given angle of attack and a given Reynolds number.

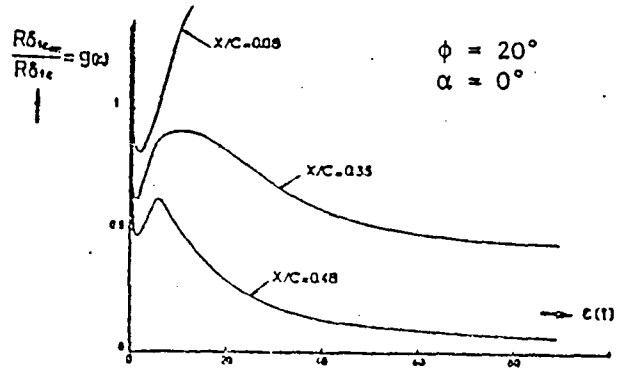

Function $g(\varepsilon)$- Boltz-Kenyon-Allen Experiments

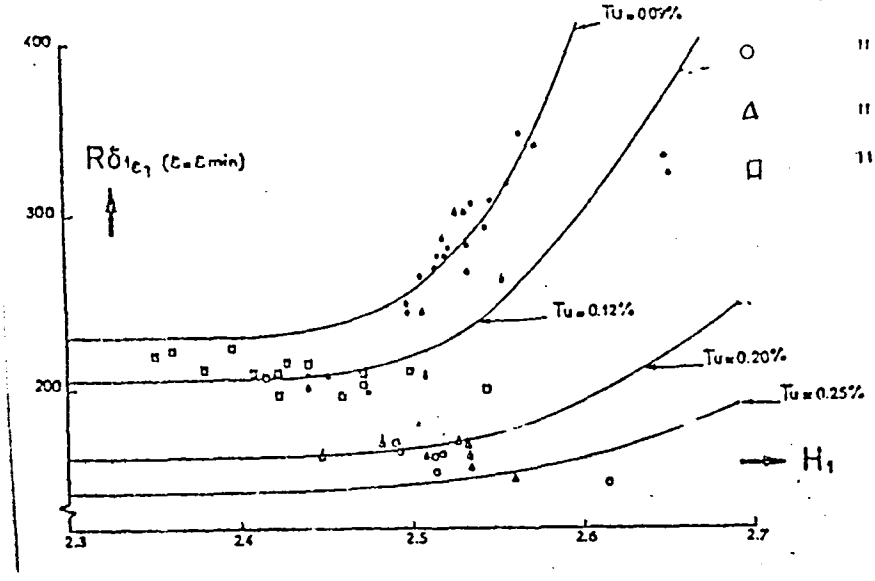

. Experiments by Boltz et al

o " Schmitt and Manie

Δ " Derat

□ " Poll

Transverse criterion

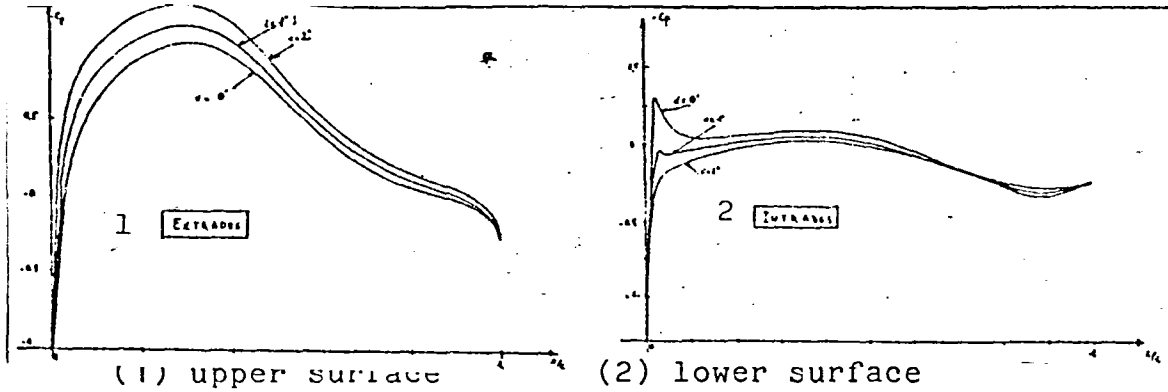

(1) upper surface (2) lower surface

Distributions of C_p (OAP01 airfoil)

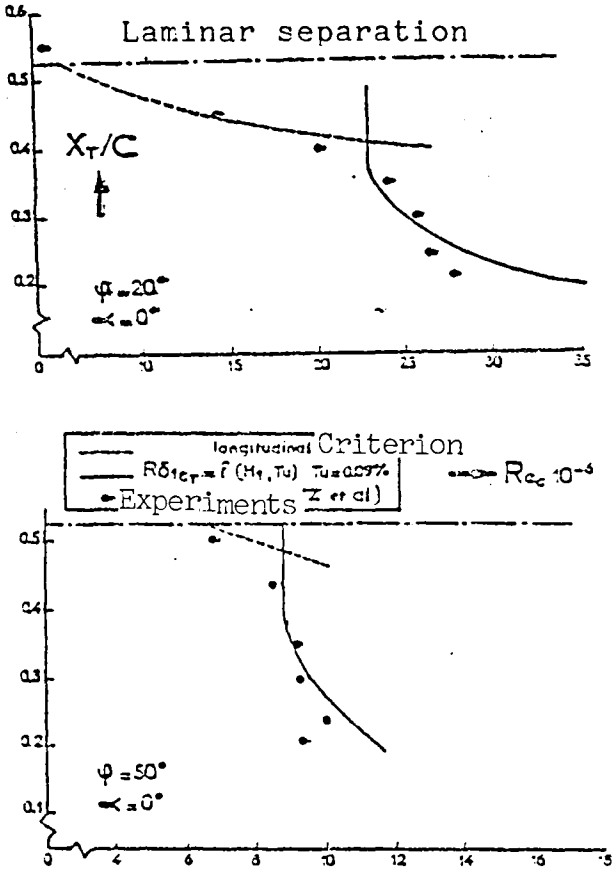

Application of the proposed criteria

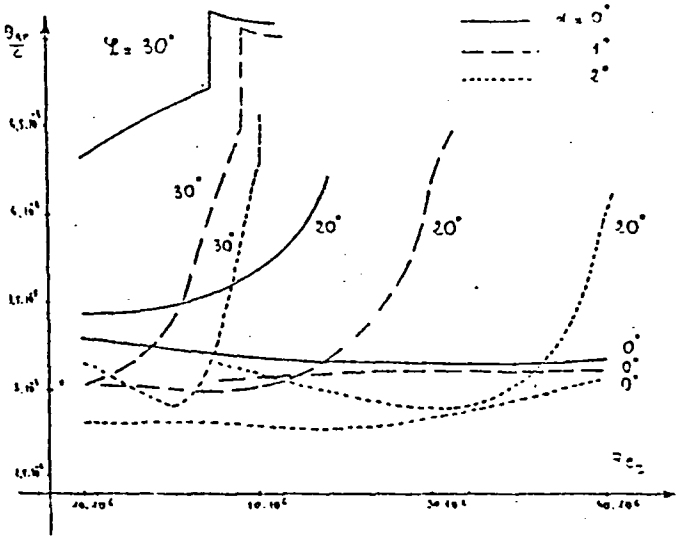

Thickness of the momentum at the trailing edge.

8.4. EXPERIMENTAL STUDIES OF THE TRANSITION ON A SWEPTBACK WING

Basic study at low speed

A first phase consisted of pursuing the systematic study of the effect of a sweep and of a Reynolds number. The sweep angle varied from 40 to 60 degrees and the normal angle of attack from -8 to -6 degrees, angles of attack for which there is no peak overspeed on the upper surface near the leading edge. For the -8° the pressure gradient is still negative whereas for the -6° angle of attack there is a velocity maximum at X/C = 0.56. 24

The position of the transition is determined by means of two methods: visualization through sublimation and Jones criterion (measurement of the stagnation pressure in the boundary layer as a function of x at a constant altitude). These two methods show that for certain configurations the variation in magnitude of the transition abscissa can reach 10 to 15% of the chord length. These variations may be due to the fact that the infinite wing assumption is not checked (wing span too small in comparison with the width of the test section) or may be due to flaws in the model (geometry, roughness). This phenomenon is accentuated by the existence of steady flow instability waves approximately aligned with the outside flow and which appear on visualizations as "streaks". The detailed study of this phenomenon is under way. It has already shown the existence of a laminar boundary layer with characteristics that undulate greatly in magnitude in the area of the streaks. Good agreement has been obtained between

the experimental determination of the wavelength and its prediction through a computation of laminar stability.

The application of two transition criteria described in Paragraph 8.1 makes it possible to predict in a satisfactory manner the location of the transition caused by the transverse instability.

Probings of the boundary layer made downstream of the transition area have shown that the downstream "undulation" of the boundary layer disappears when the latter becomes turbulent. The experimental values of the integral thicknesses of the boundary layer and of the friction coefficient are compared against a complete computation of the boundary layer, from the leading edge to the trailing edge. This computation makes it possible, in particular, to describe the transition area thanks to the intermittence method previously described.

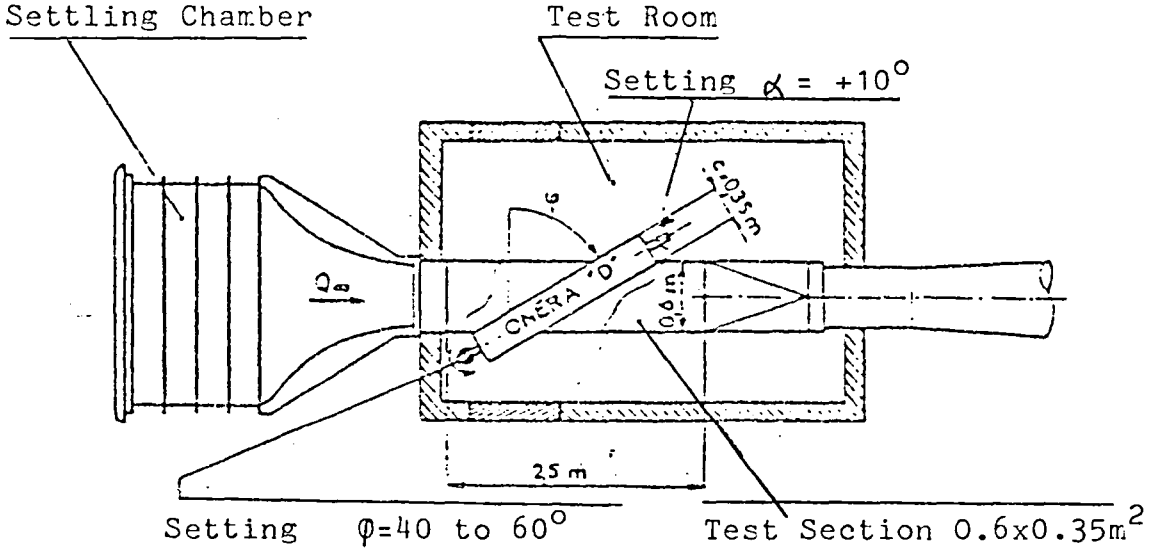

EXPERIMENTAL SET-UP

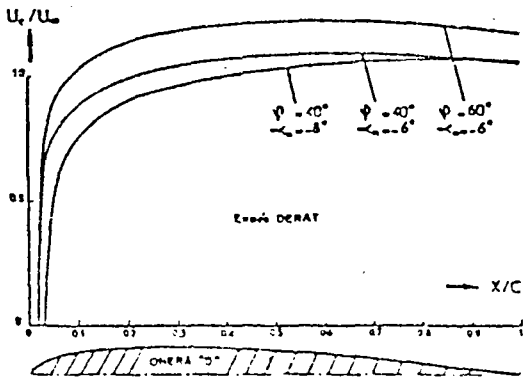

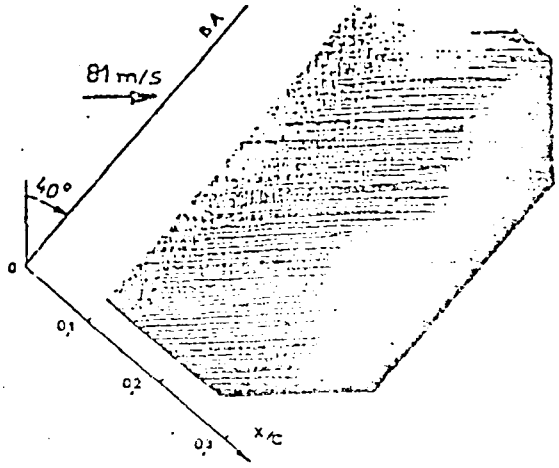

Velocity distributions on the upper surface

Visualization of the streaks

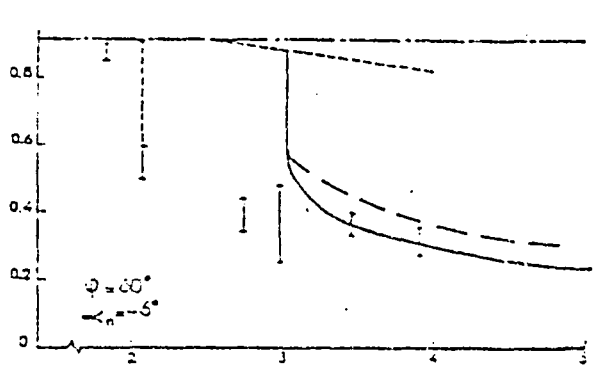

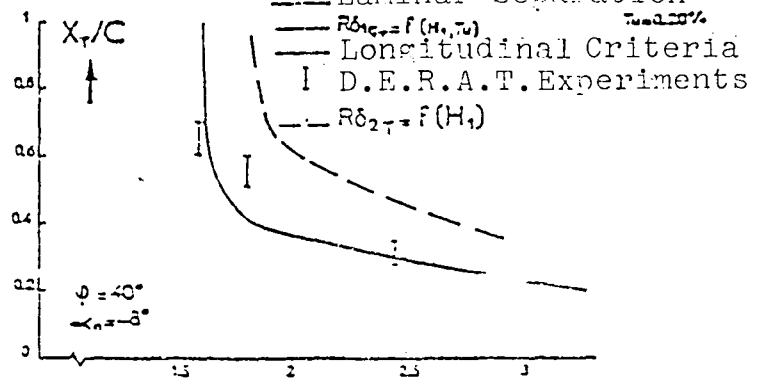

Application of transition criteria, comparison against experiments

. Experiment (Z=391mm) . Experiment (Z=391mm)

Computation ($X_T/C = 0.25$) Computation ($X_T/C = 0.25$)

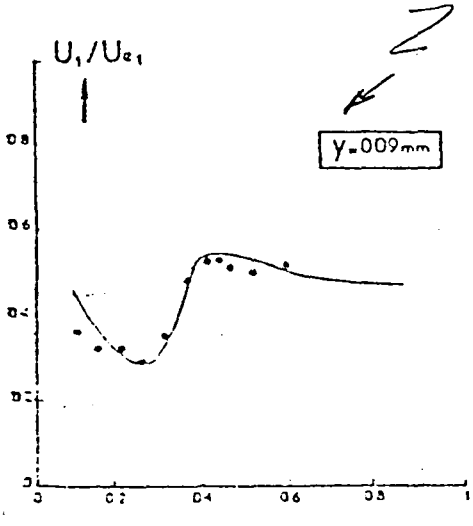

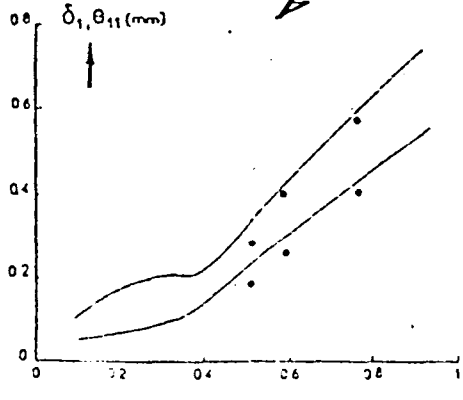

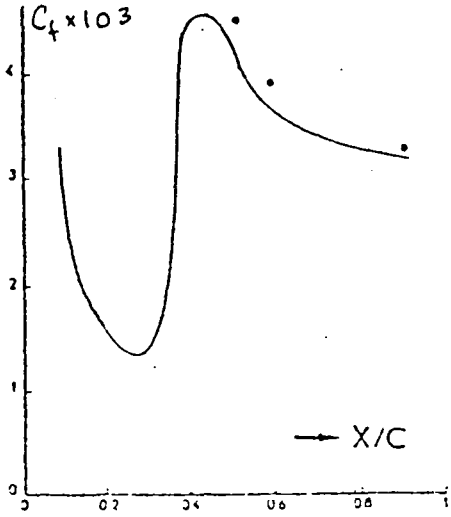

Jones Criteria Integral thicknesses Friction Coefficient

Transition over a sweptback wing in transonic regime

A few preliminary tests aimed at obtaining data pertaining 26
to the location of the transition over a sweptback wing in a moderately compressible flow have been performed at the T2 wind tunnel, operating at ambient temperature.

They involve the "variable sweep" wing of airfoil LC 100 D with a chord length of 100mm; the results pertain primarily to the 45 deg. sweep angle.

The transition was determined on the upper surface by means of visual visualizations using an oil film and performed at various negative angles of attack, with the upstream Mach number capable of reaching 0.8.

We show the observed location of the transition as a function of the chord Mach number for various angles of attack, as well as the corresponding results obtained by means of a computation of the transition using the transition criterion from transverse instability of incompressible flow.

Despite the uncertainty occurring in the determination of the transition through visualization at the surface, the motion of the transition matches the one indicated by the criteria; we clearly note the forward motion of the transition when the angle of attack becomes more negative, a forward motion caused by the accentuation of the negative pressure gradients and the corresponding increase of the boundary layer transverse flow and its stabilizing effect.

8.5. - CONDITIONS FOR THE APPEARANCE OF THE VORTEX REGIME OVER A SWEPTBACK WING

Tests over the sweptback wing used in the basic study of the transition at a low speed have been devoted to both the study of the bursting of the leading edge transition bulb and the appearance of the vortex regime at high angles of attack.

The passing from a flow with a leading edge bulb to a vortex regime has been revealed through the measurement of the pressures along the contour and through visualizations along the surface during a gradual reduction of the Reynolds number at a fixed angle of attack.

The extent of the area affected by the bulb and the vortex flow area as a function of the Reynolds number could be determined.

It is to be noted that artificially tripping the transition, performed during tests at a rather low Reynolds number, resulted in the suppression of the vortex regime.

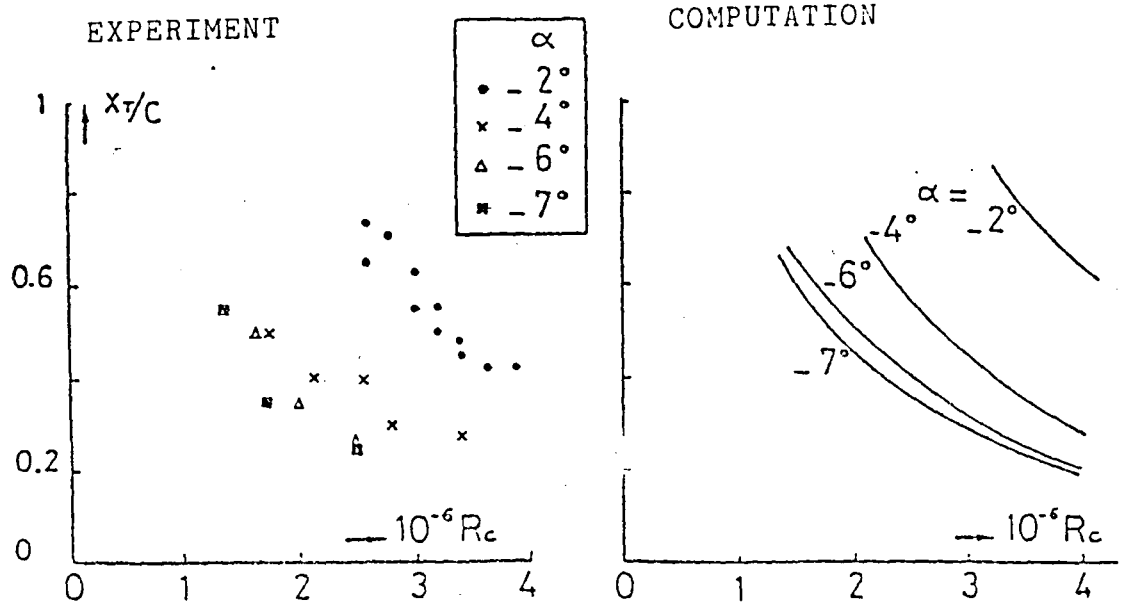

TRANSITION THROUGH TRANSVERSE INSTABILITY IN TRANSONIC REGIME

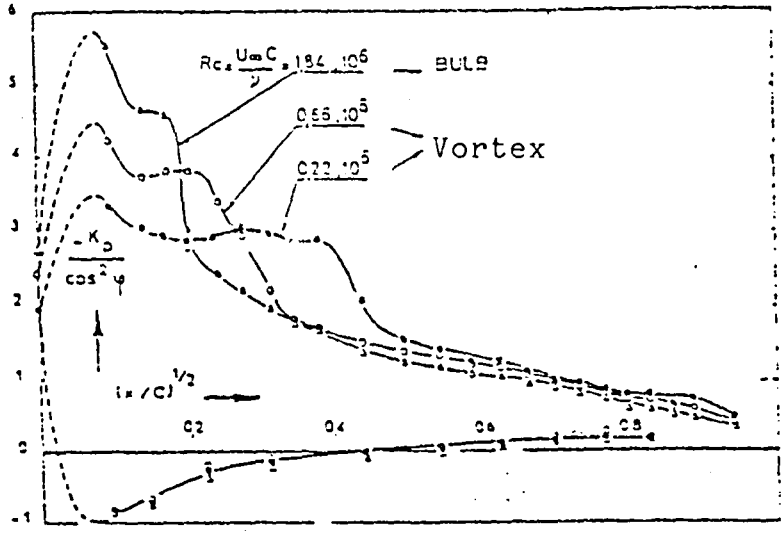

PRESSURE COEFFICIENT DISTRIBUTIONS

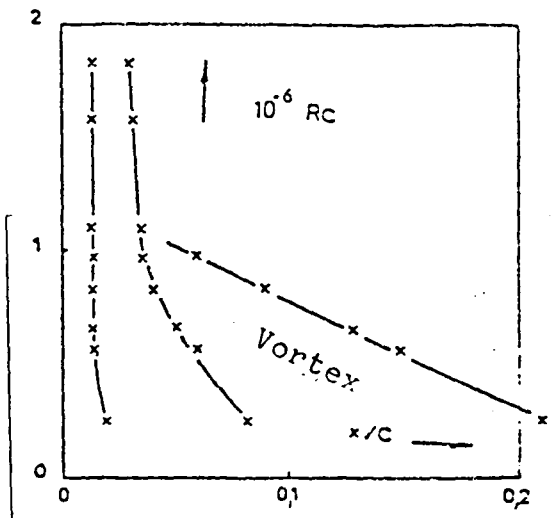

DOMAINS WHERE THE VORTEX AND BULB EXIST

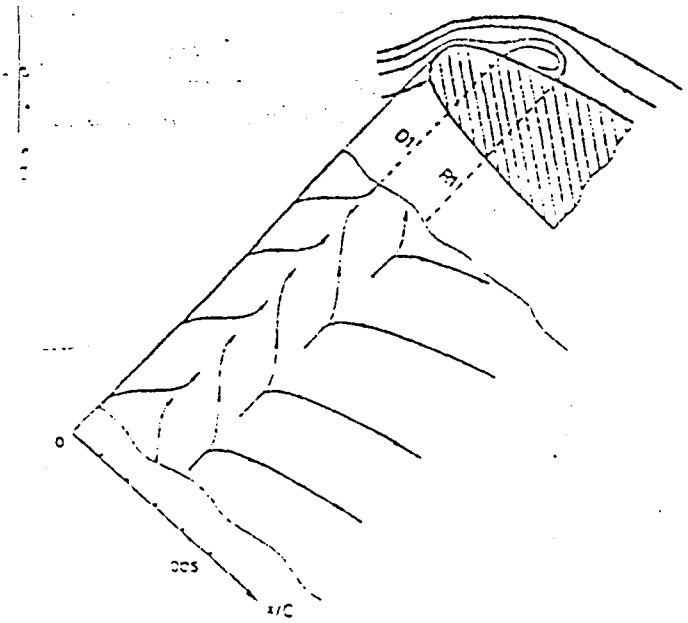

FLOW DIAGRAM: BULB ONLY

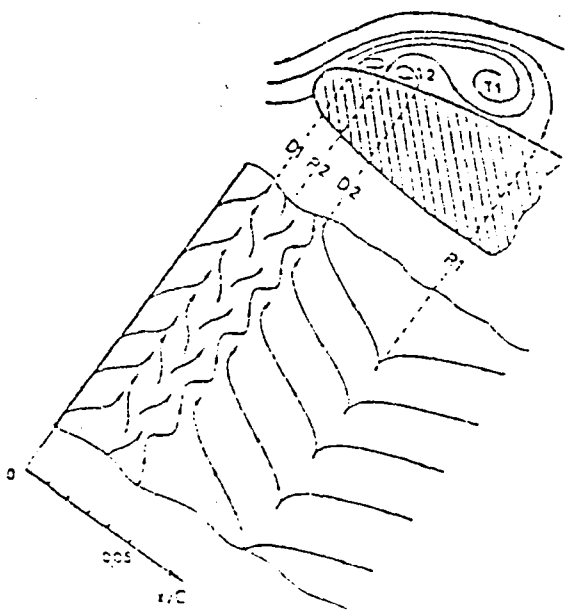

FLOW DIAGRAM: BULB AND VORTEX

9 - DETAILED STUDY OF THE CAST 7 AIRFOIL AT THE T2 WIND TUNNEL

This experimental study dealt with the detailed analysis of the viscous flow regimes (boundary layer and near wake) near the trailing edge of the CAST 7 airfoil with a chord length of 200 mm, mounted between adjustable walls inside the test section of the T2 wind tunnel. 28

All of the tests were performed with a transition tripped at 7% of the chord, with a total pressure close to 1.7 bars, at ambient temperature.

Two main configurations were considered for the tests:

- a Mach number varying between 0.75 and 0.79 around the divergence Mach number at a zero incidence angle
- an angle of attack varying between 1 and 3 degrees at M_0=0.7, a configuration that causes the appearance of a local separation of the boundary layer at the bottom of a shock located between 20 and 40% of the chord.

The measurements made inside the boundary layer were made primarily near the trailing edge, over the lower surface and particularly on the upper surface of the airfoil, a few explorations defining only the conditions upstream of the shock.

The evolution of the displacement thickness and of the momentum thickness is given as an example of one case of the first configuration; we note a very quick thickening over the rear portion of the airfoil where the boundary layer develops into a velocity profile approaching a separation profile.

A boundary layer computation using the experimental pressure

distribution has been performed; there is good agreement with the experiment up to 75% of the chord; a divergence then appears, particularly in the displacement thickness, and has led to a discussion on the possible effect of secondary factors (airfoil curvature, boundary layers on the side walls) to take into consideration in computations. However, we must emphasize the difficulty of accurately measuring a boundary layer close to separation near the trailing edge (vibration of the probe, inaccuracy in locating the surface).

An example of stagnation pressure distributions measured at various Mach numbers in the near wake is also given; it clearly reveals the two areas of pressure drop originating, respectively, from the boundary layer and the shock wave, the second increasing clearly with the Mach number , that is to say in fact, with the strength and width of the shock wave.

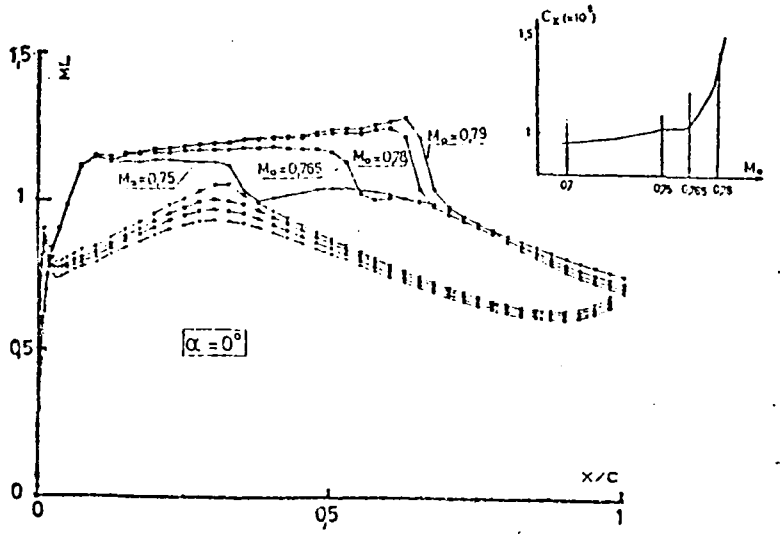

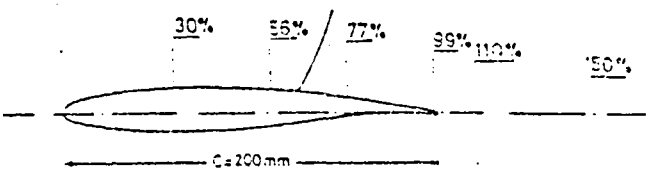

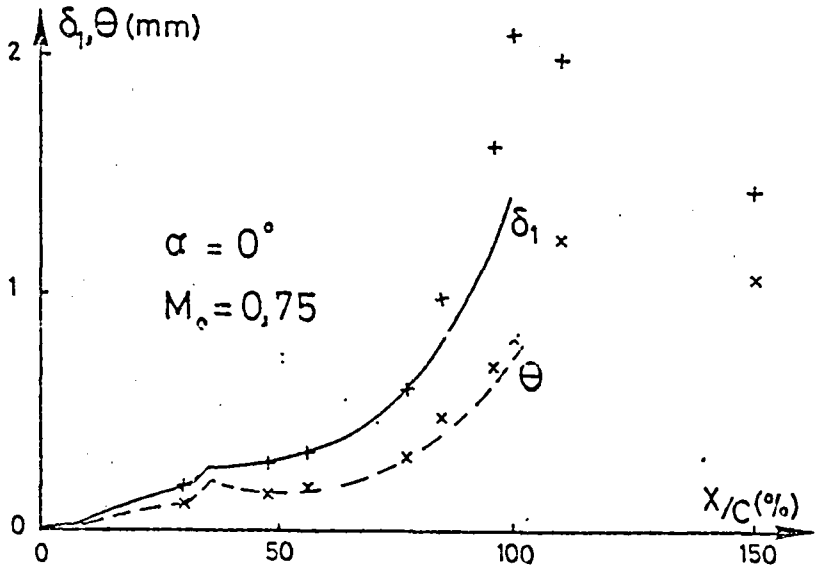

Displacement thickness and momentum of the boundary layer on the airfoil.

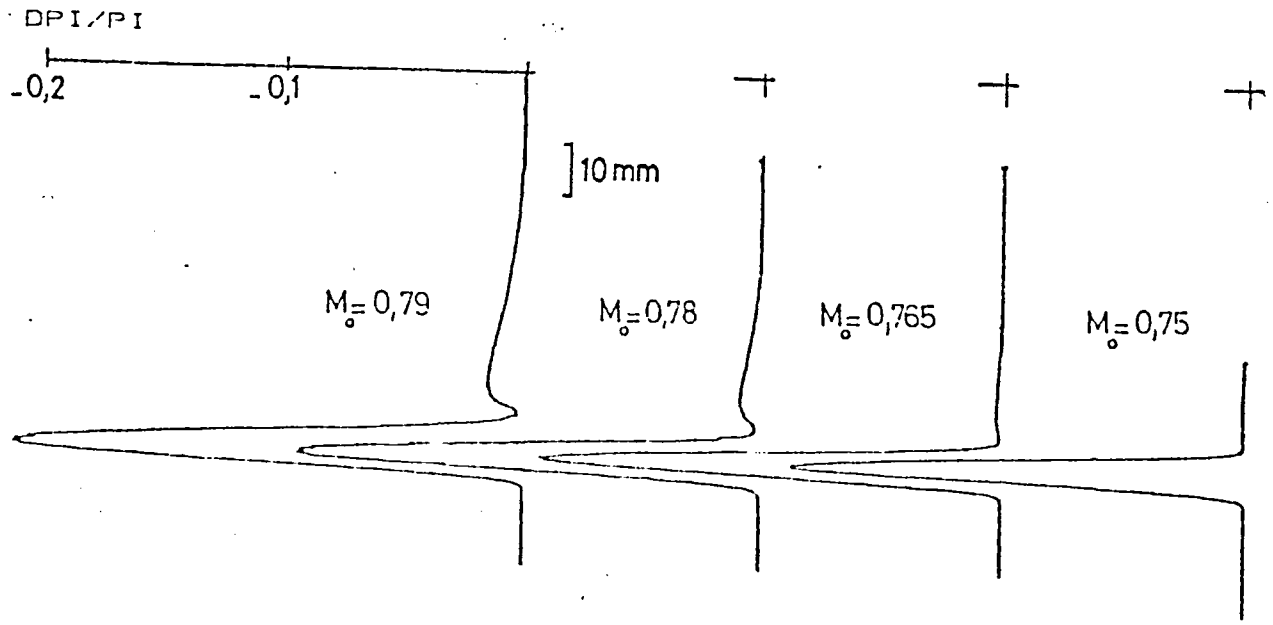

Wake in X/C = 110% $\alpha = 0^{\circ}$

10 - SHOCK-BOUNDARY LAYER INTERACTION WITH TRANSITION AT THE BOTTOM OF THE SHOCK

This experimental study dealt with the analysis of the behavior of the boundary layer and its interaction with the recompression shock wave in the case where the boundary layer, initially laminar, becomes turbulent through transition inside the interaction region. 30

The tests were performed at the T2 wind tunnel, operating at an ambient temperature, using the model of the CAST 7 airfoil with a chord length of 200 mm.

A first step consisted of defining the cases to be studied, searching for configurations providing a laminar boundary layer up to the shock; it involves pressure distributions that have, at their beginning, an area with a negative gradient stabilizing the boundary layer followed by an area with a zero or slightly negative gradient up to the shock.

We chose to set the shock wave at about 50% of the chord; by changing the angle of attack and the Mach number, we obtain, ahead of the shock, a flow with a Mach number varying from 1.18 to 1.40, thereby studying different strength values of the shock wave.

The distributions of the local Mach number show a two-step recompression with a constant pressure plateau between the two steps which are characteristic of a lambda shock wave and of the existence of a boundary layer at the beginning of the interaction; the second recompression step, much clearer and much larger, is on the other hand characteristic of a turbulent boundary layer.

Surface visualizations using an oil film have in fact shown that the laminar boundary layer separates, transitions and returns to the surface in a turbulent flow near the interaction.

Measurements performed inside the boundary layer at the abscissa value X=0.32 have confirmed that the boundary layer is laminar upstream of the shock; its characteristics, particularly its displacement thickness, depend little on the magnitude of the local Mach number.

For each of the configurations, the boundary layer after the shock and its development as far as the trailing edge have been described by means of measurements performed at abscissa values of 0.65, 0.80 and 0.95.

It is therefore clear that the boundary layer is turbulent after the shock and that the thickening that it has undergone while crossing is greater with a higher upstream local Mach number. The displacement thickness then increases considerably down to the trailing edge, and even more so when the case considered involves a stronger shock.

These experimental results provide the basis for checking a computation method that remains to be established and in which the effects of a transition of the boundary layer on the boundary-shock wave interaction phenomenon are taken into account. The dashed line plotted on the figure only represents a very rough computed estimate, using the experimental distribution of the pressures with the hypothesis of a transition at the location of the shock; relatively close to the experiment with the weakest shock, the results of this

computation become entirely unacceptable as soon as the strength of the shock increases.

Legend:

(1) $M_{upstream} = 1.40$

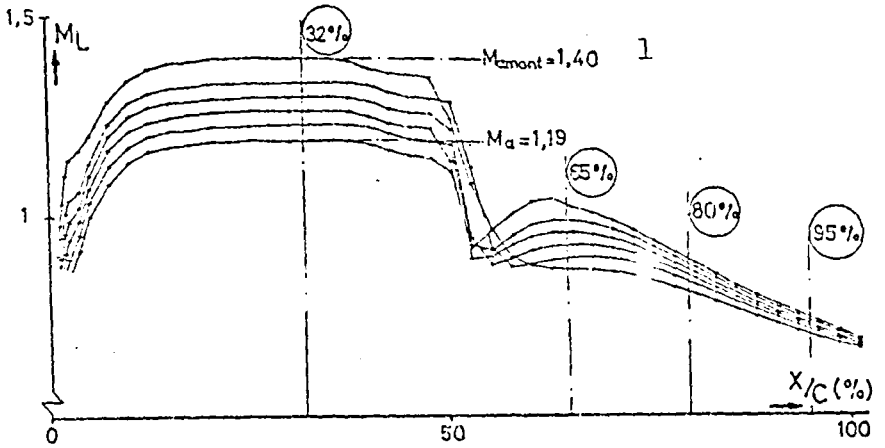

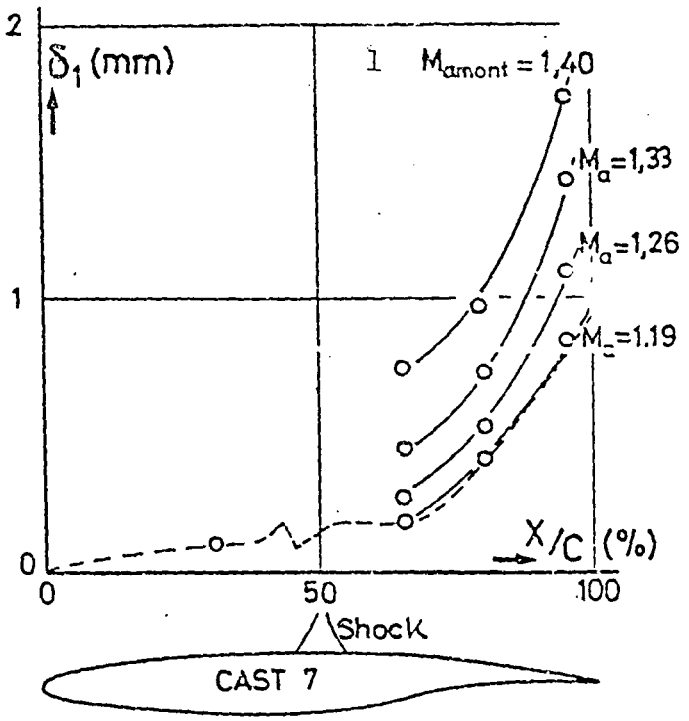

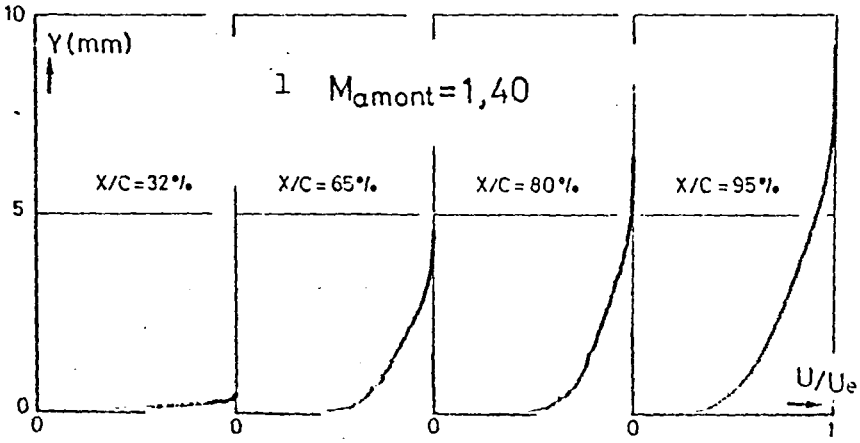

11 - ADJUSTING THE WALLS IN A TRANSONIC WIND TUNNEL

11.1. - ADJUSTABLE WALLS FOR THE CRYOGENIC OPERATION OF T2

In view of the cryogenic modification of T2, we were led to 32
equip the wind tunnel test section with new deformable walls operating at a low temperature.

We chose to use thermally conducting metal sheets; thermal flow computations show that it is possible to have their temperature equal that of the flow over periods of time that are entirely compatible with the duration of the blast, at least for a small thickness, and provided the effect of the straightener vanes is reduced to a minimum.

The new adjustable walls of T2 are thus made of Invar, a material with a small coefficient of expansion, mechanically strong at a low temperature; they have a thickness of 3 mm; the straightener supports are notched, with holes of a size computed to reduce their thermal inertia to the maximum extent.

11.2. - OPTIMIZATION OF TECHNIQUES FOR ADJUSTING THE WALLS

Four improvements were added to the original method:

- Optimization and extension of the computation mesh to predict with greater accuracy the outside field using a formula by Green.
- Determination of the velocity at infinity by cancelling the velocity correction, the weighing procedure giving greater weight near the model which, in fact, defines the Mach number of the test.
- Introduction of a projection making it possible to go

through the curved wall to make measurements along the straight reference line along which the outside field is computed using Green's formula.

- Extrapolation of the test zone up to x = ± 40 m, by means of a reference model (with distributed points) with a connection to the four outside experimental values.

New numerical methods (finite elements, small transonic perturbations) have also been applied to compute the outside field in cases where the local Mach number at the wall is close to 1.

An analysis of the diagram of a velocity field through the use of a pannel method currently constitutes a first theoretical approach for the modification for three-dimensional flow.

11.3. - EFFECT OF THE SIDE WALL BOUNDARY LAYERS

A few tests of the CAST 7 airfoil between adjustable walls have revealed these effects in two ways:

- a suction at a variable rate has made it possible to modify the thickness of the boundary layers on the upstream side walls and their evolution inside the pressure gradients near the model;
- the map of the displacement thickness around the airfoil, determined from computations performed over different streamlines, has made it possible to build a detailed compensation over the cross-section, thanks to which the effects of the boundary layers seem to be greatly resorbed.

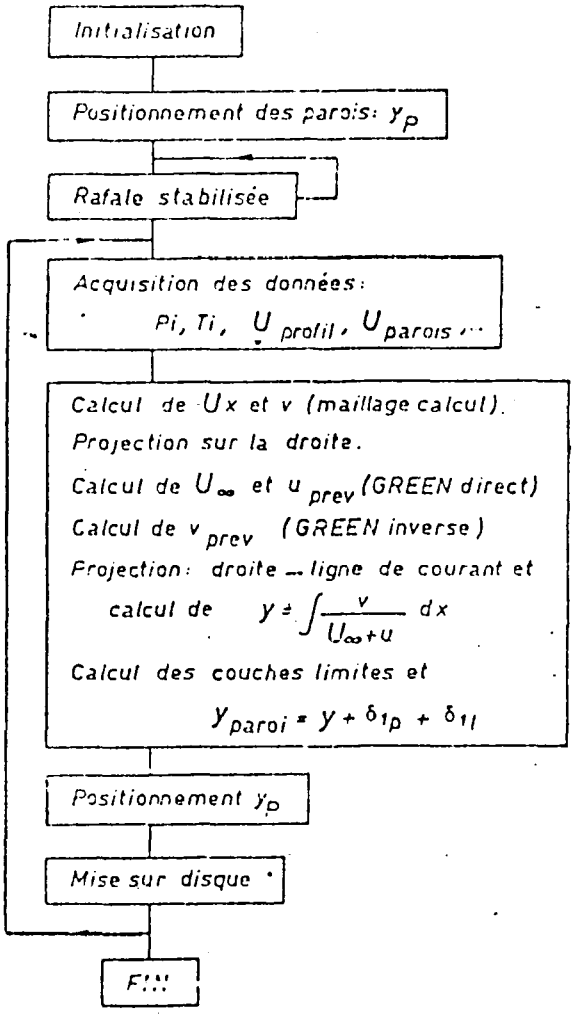

[Initiation

[Positioning of the walls: y_p

| Stabilized air blast

[Data Acquisition
P_i, T_i, $U_{airfoil}$, U_{walls}

[Computation of Ux and v (computation mesh)
Projection on straight line
Computation of U and u_{prev} (Green direc
Computation of v_{prev} (Green inverse)
Projection: straight line → streamli
and computation of
Computation of boundary layers and
$y_{wall} = y+_{1_p}{}^{+}\ 1$

[Positioning y_p

[Recording on disk

[END

- Flow diagram for the modification

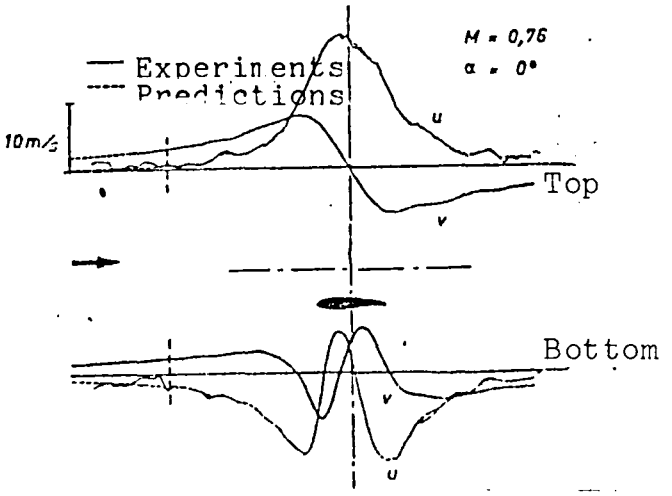

- Comparison of the u's and v's before and after Green.

Legend:

(1) Standard test

(2) 5% suction

(3) Compensated side boundary layers

(4) Suction

(5) Surface boundary layer

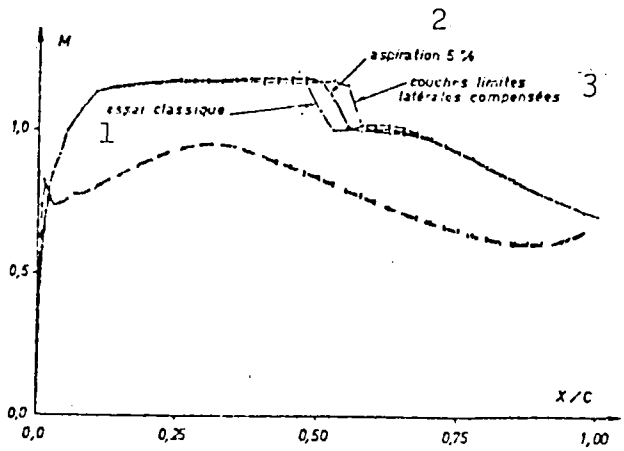

Effect of the lateral boundary layers on the airfoil.

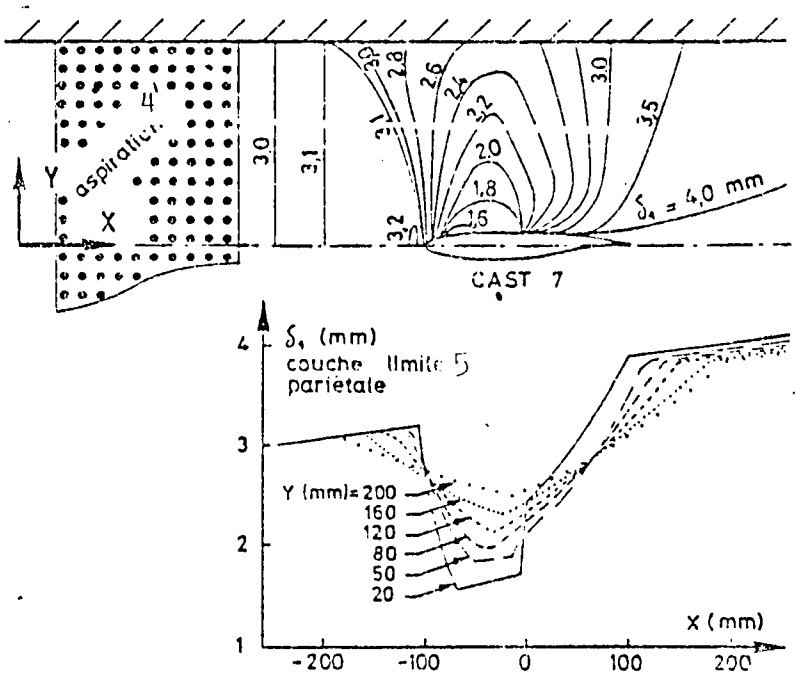

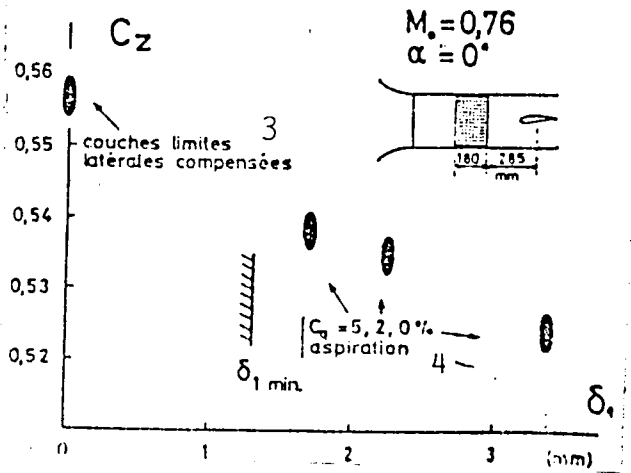

12 - DESCRIPTION OF THE CRYOGENIC FLOW INSIDE T2

12.1. - THERMAL GRADIENTS INSIDE THE TEST SECTION

A new analysis of the temperature distribution in space inside the test section was performed, a detailed measurement using a shielded thermal probe examining the region close to the wall in particular. 34

The transverse distribution shows a uniform central area bordered by warmer flow areas that are clearly greater than the dynamic boundary layer; their size is practically independent of the test temperature and the difference between the wall temperature and the stagnation temperature at the center does not exceed about 12 degrees Centigrade.

12.2. - TEMPERATURE AND PRESSURE FLUCTUATIONS

(Tests at M = 0.8, Pi = 2 bars, start of a throat)

Pressure fluctuations: They are measured up to a frequency in the order of 10 kHz by means of a Kulite sensor mounted on the wall of the test section (reduced frequency: $n = \frac{fh}{U}$; $\int_0^{n\,max} F_p(n)\,dn = \frac{p'^2}{(\frac{\rho}{2} U^2)^2}$)

At the ambient temperature, the spectrum is very close to the one that we had obtained before the circuit was modified. At a low temperature, we note a slight rise of the fluctuation level which is certainly linked to the thermal turbulence.

Temperature fluctuations: They are measured inside the settling chamber, up to a frequency in the order of 50 Hz, by means of a "cold wire". The average quadratic value of the fluctuation goes from 0.03K at ambient temperature to

0.14K at Ti = 100K. Involving low frequencies, part of the fluctuation may come from the temperature control which is performed in steps; the homogeneity of the mixture of warm driving air and the driven cold gas may also be involved.

T2.3. - APPEARANCE OF PARTICLES - GAS CONDENSATION LIMIT

Using the diffusion of the light emitted by a laser beam, the thresholds when the particles appear as a function of temperature and the gas condensation limit were determined (tests at Pi = 2 bars).

The recording of the signal from the photomultiplier and the measurement of the pressure drop in the filter at the entrance to the settling chamber make it possible to distinguish three phenomena:

- appearance of ice particles at a temperature in the order of 250K then appearance of carbonic snow particles at a temperature in the order of 135K; these particles "trapped" by the filter give rise to a greater pressure drop;
- very large flow of particles at low temperature (Ti = 93K); the pressure and temperature conditions inside the test section make it possible to attribute it to the condensation of the air-nitrogen mixture; there appears that a total temperature of 100K can be easily obtained for transonic tests up to a total pressure reaching 3 bars.

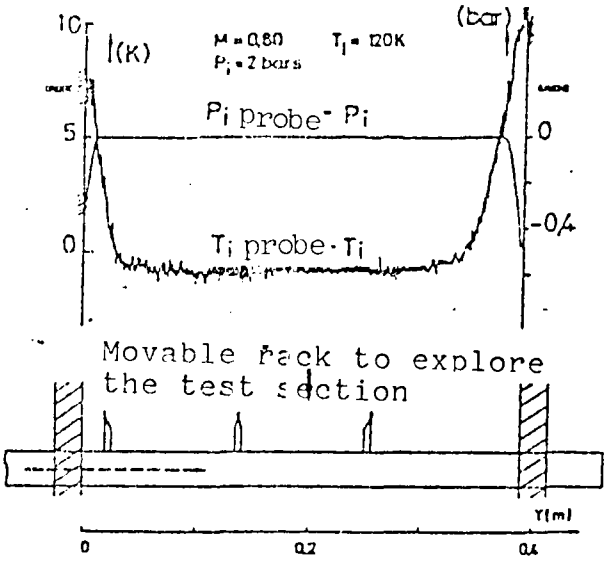

Example of transverse temperature distribution inside the test section during a test at Ti=120K, M=0.8 and Pi=2bars.

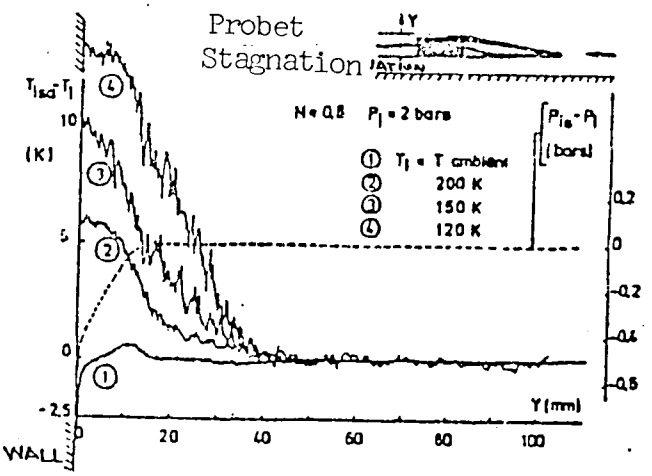

Stagnation temperature measurements near the side wall.

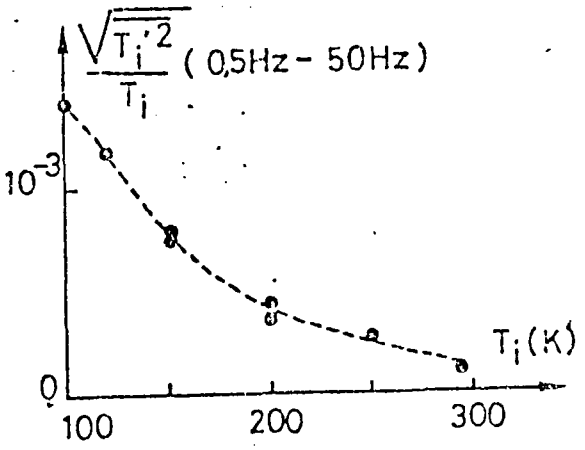

Evolution of the overall level of thermal fluctuation over the 0.5Hz to 50Hz frequency band as a function of the test temperature

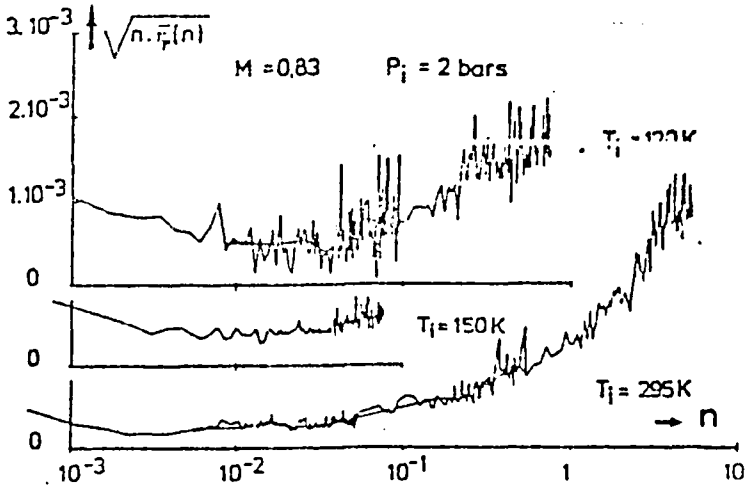

Description of the pressure distributions at the test section wall.

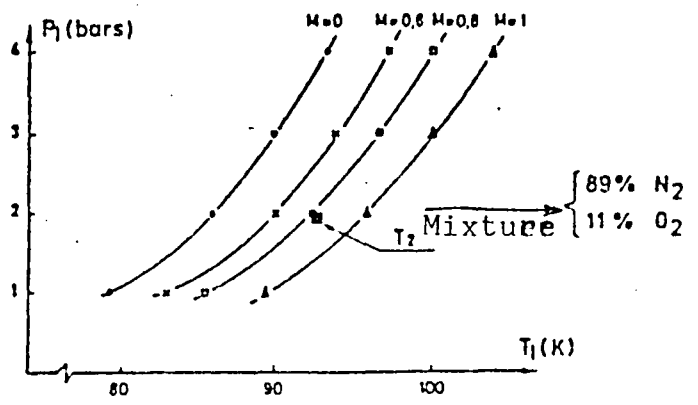

Operating limit near the low temperatures, limit associated with the condensation phenomenon of the fluid inside the test section.

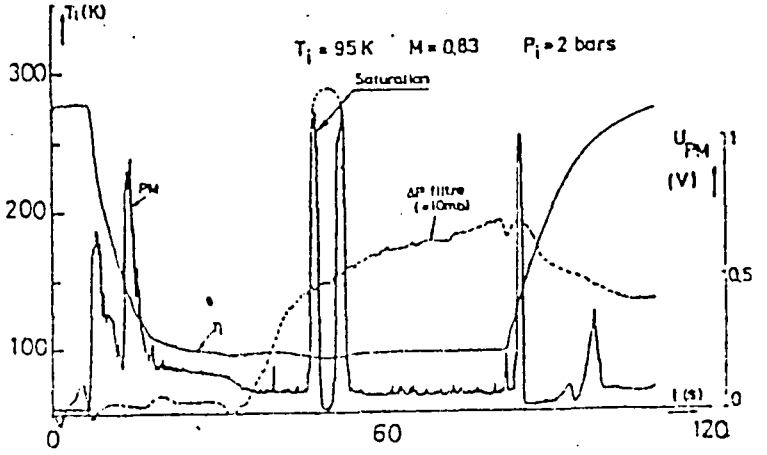

This figure shows the appearance of particles during an air blast at a low temperature Ti=95K.

13 - PREPARATION OF AIRFOIL CRYOGENIC TESTING AT T2

13.1. - SEQUENCE OF EVENTS FOR A CRYOGENIC BLAST

The solution retained to reach a thermal equilibrium consists of precooling the airfoil before inserting it into the test section. A cryogenic blast will thus include several sequences which will already have been perfected during tests conducted at T2, without a model for the time being. 36

- during the first step, a flow at a low Mach number and at a low pressure but at a nominal temperature is initiated: the wind tunnel being started at the ambient temperature, a flow of liquid nitrogen at three times the equilibrium value is injected, causing the temperature to drop quickly; it is then gradually reduced, the computer providing control to reach the desired temperature level.
- the second step consists of introducing the precooled airfoil into the test section.
- during the third step, the Mach number and the pressure are increased up to the values of the test itself through programmed action on the flow of the air entering and on the air exhaust rate. The temperature is maintained at a constant level through an increase of the nitrogen flow rate matching that of the flow of the air entering.
- the fourth step, maintains the test parameters at nominal values thanks to a closed-loop pressure and temperature control; it is during this step, where the conditions have been reached, that the measurements will be made on the airfoil.

13.2. - DESIGN OF A WING AIRFOIL MODEL (CAST 7 airfoil)

The design and construction of a model of the CAST 7 airfoil for cryogenic tests at T2 resulted from studies performed by the Direction des Grands Moyens d'Essais (Directorate of Major Testing Means) of ONERA, studies bearing on the selection of the material most suitable at low temperatures and on the set-up minimizing the thermo-mechanical stresses. The material retained is a MARVAL 18 "Maraging" steel with a high nickel content.

The model is composed of three parts (leading edge; upper surface and trailing edge; lower surface) which are welded together; the empty area separating them as well as the grooves for the pressure and temperature tubes are filled with a "nickel felt" in order to insure homogeneity of the thermal mass. A stub on the right side connects the airfoil to the system for moving the pre-cooling unit. A stub on the left side makes it possible to lock the model when it is placed inside the test section.

The chord length of the airfoil is 150mm; it is equipped with 103 pressure taps, the majority with a diameter of 0.3mm; in order to solve problems associated with the possibility of tripping the transition, 32 taps with a smaller diameter (0.8mm) are installed in the area of the leading edge where the boundary layer is thin.

Temperature control is provided by 18 copper-constantan thermocouples placed at a depth of 1mm under the airfoil surface. The ten thermocouples are distributed along the center chord from the upper to the lower surfaces; the others are installed

along the wingspan.

13.3. - PRECOOLING THE AIRFOIL

The preliminary phase of the test of a wing airfoil in a cryogenic flow therefore consists of cooling the model to bring it to a temperature sufficiently close to that of the flow inside which it will be introduced. 38

The solution retained is that of cooling by using a cold gas flow; a simple set-up having been bench-tested, it was used as a foundation for the precooling apparatus built for testing airfoils in a cryogenic regime in the T2 wind tunnel.

This apparatus consists of a closed circuit operating at an atmospheric ambient pressure and adjacent to one of the side windows in the test section; it includes two parts:

- a cooling section hosting the airfoil and equipped with the moving device which will make it possible to introduce it inside the test section of the wind tunnel,
- the circuit itself, equipped with the nitrogen-injection system (two small-diameter nozzles), the driving fan, the exhaust, and the temperature control through a heater.

The apparatus was first perfected in the presence of a reference model made of an aluminum alloy; a satisfactory check of the time periods needed to reach different temperature levels and cooling uniformity was made.

It was then used to performed the precooling tests of the CAST 7airfoil planned for the cryogenic tests at the T2 wind tunnel.

The examples of recordings given below show that the center

section of the model (region A) reaches the temperature of the flow in about ten minutes; only the thermocouples located at 20 mm from the side stubs (region B) show differences caused by the effects of conduction, differences that should then disappear for the most part during the cryogenic test itself.

We were also able to check the good behavior of this model which is of a new design, being made of a steel with a high nickel content and cooled for the first time during these tests. No appreciable deformation was recorded despite the application of temperatures dropping as low as 120K. Of course, proper behavior remains to be confirmed when the model is also subjected to aerodynamic stresses during testing.

Legend:
(1) injection of airfoil
(2) opening of digital valve (%)
(3) analog valve pre-set at 38%

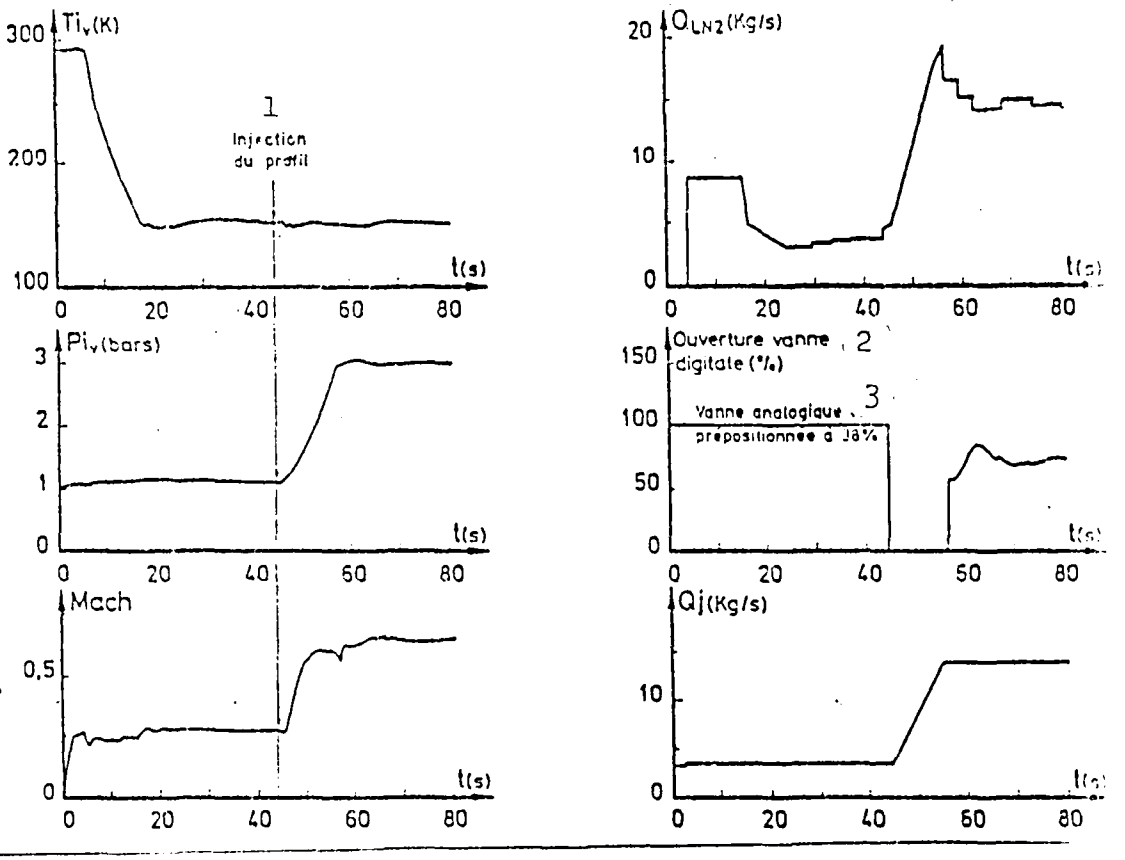

32 taps 0.1mm dia. 71 taps 0.3mm dia. 18 thermocouples

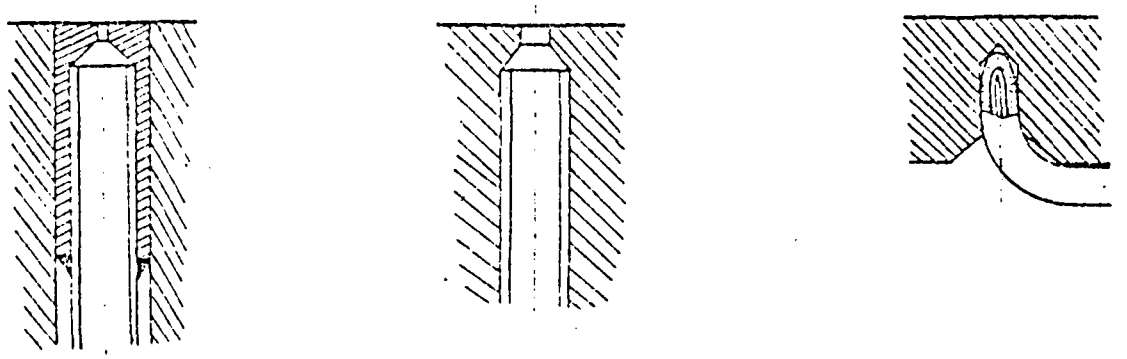

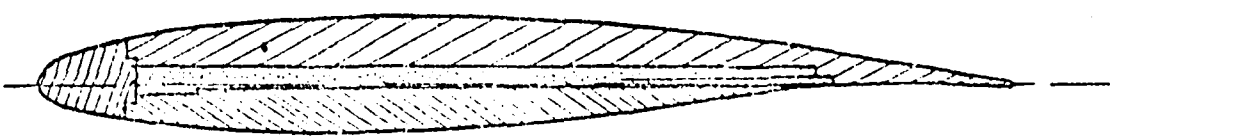

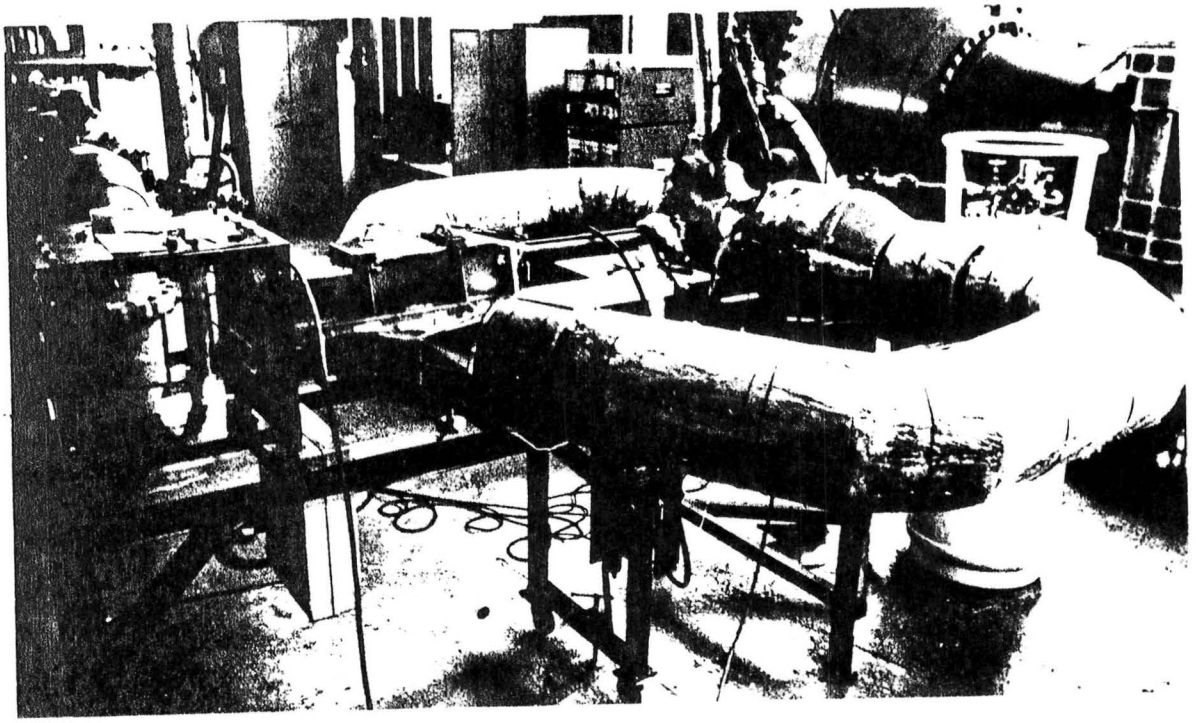

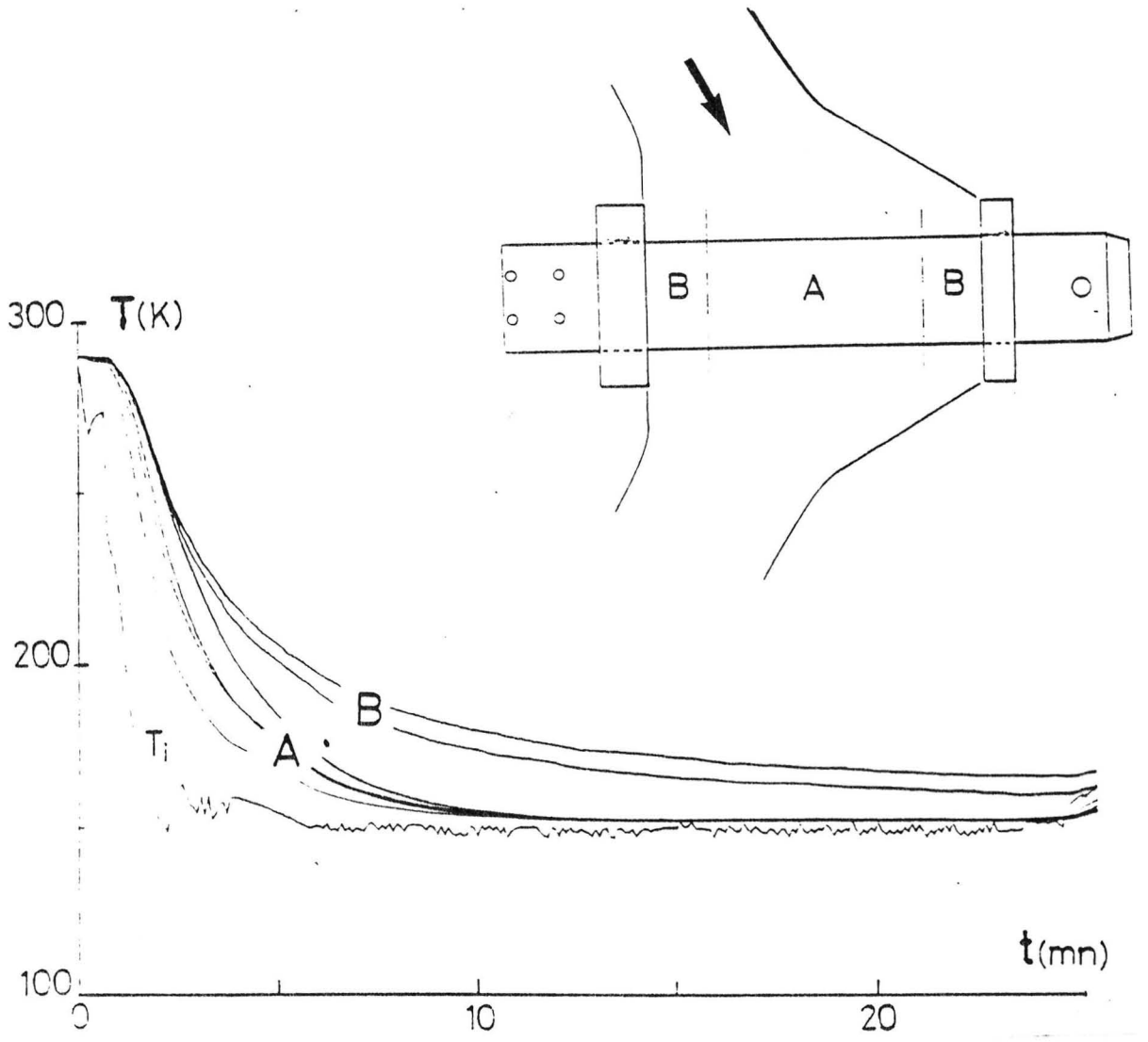
B
A
B
300
T(K)
200
100
Ti
A
B
t(mn)
0
10
20

14 - PROBLEMS ASSOCIATED WITH THE USE OF CRYOGENIC WIND TUNNELS

14.1 - INSTRUMENTATION AND MEASUREMENT TECHNIQUES

Pressure and temperature probes: In addition to a synthesis summarizing the results acquired with the various pressure sensors that we were led to test in a cryogenic environment, efforts were made to define and use miniaturized probes; a small-size probe (diameter of 4mm) and with a larger bandpass was built. 40

A shielded stagnation temperature probe, with a recovery factor close to one, was also built; its utilization inside the wind tunnel T2 was very valuable when measuring the distribution of temperatures inside the wall boundary layer in the test section.

Optical detection of particles: Preliminary tests inside the wind tunnel T'3 have shown the possibility of detecting the presence of particles inside the flow by using the light emitted by a low-power laser and diffused by the particles; the optical viewing capability using two side windows that reduce the formation of frost was necessary for "long" tests at T'3. The utilization of the system in the T2 wind tunnel has made it possible to define the appearance of the different types of particles, and to define the gas condensation limit in that tunnel.

Surface friction gauges: The DERAT hot wire and hot film gauges were designed and tested for mesuring the surface friction in low-temperature flows. A few tests conducted at T2 on a reference model (flat aluminum plate) have shown

the feasibility of such surface measurements. The quartz rod gauge, capable of providing unsteady flow values was tested inside the enclosure; after a few modifications to the mounting onto the support, we expect to be able to use it to define, in particular, the nature of the boundary layer and of the transition in the cryogenic mode.

14.2. - T'3 CRYOGENIC WIND TUNNEL WITH FAN

The improvement of the operation of the small T'3 cryogenic facility was pursued with the installation of a new exhaust casing now located right after the test section outlet; the suction of the boundary layer at the entrance to the diffuser contributes in a major fashion to a reduction in the pressure drop of the circuit and to the expansion of the operating domain of the wind tunnel.

The preparation of a two-dimensional set-up particularly designed for the study of the detection of the transition in a cryogenic environment was performed; this set-up includes a simplified model composed of a flat plate with an unsymmetrical leading edge and an adjustable flap, and computed to minimize overspeed at the seam.

The test section is equipped with simplified deformable walls that make it possible to avoid blockage and to adjust the pressure distribution along the flat plate. A system for the longitudinal and vertical exploration of the flow is planned, particularly for flat plate boundary layer measurements.

Detailed view of side windows

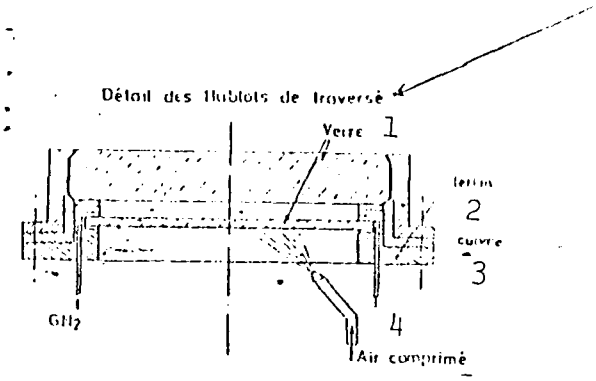

Legend:

(1) Glass

(2) Teflon

(3) Copper

(4) Compressed air

(5) Side walls

(6)

(7) Lenses

(8) Photomultiplier

(9) Diaphragm

(10) Filter

(11) Output (voltmeter)

(12) Regulated supply,
High voltage

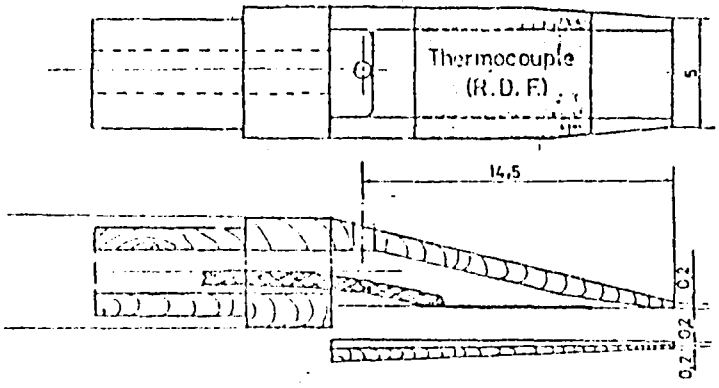

Temperature probe

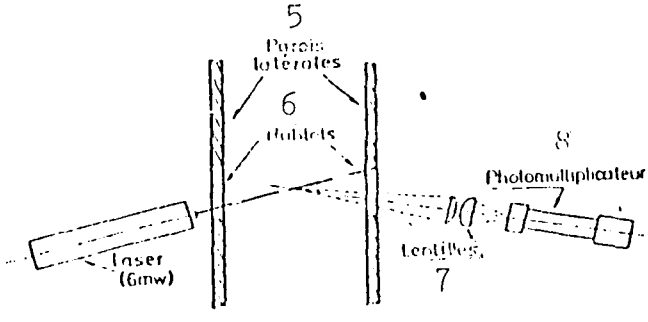

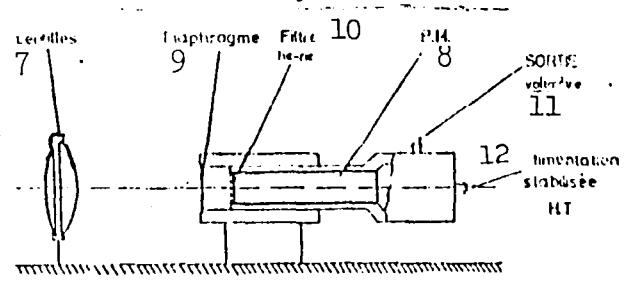

Optical detection of particles

Legend:

(1) Low velocity exhaust

(2) High velocity exhaust

(3) $M_{test\ section}$

(4) Test section

(5) Throat

(6) Liquid nitrogen injector

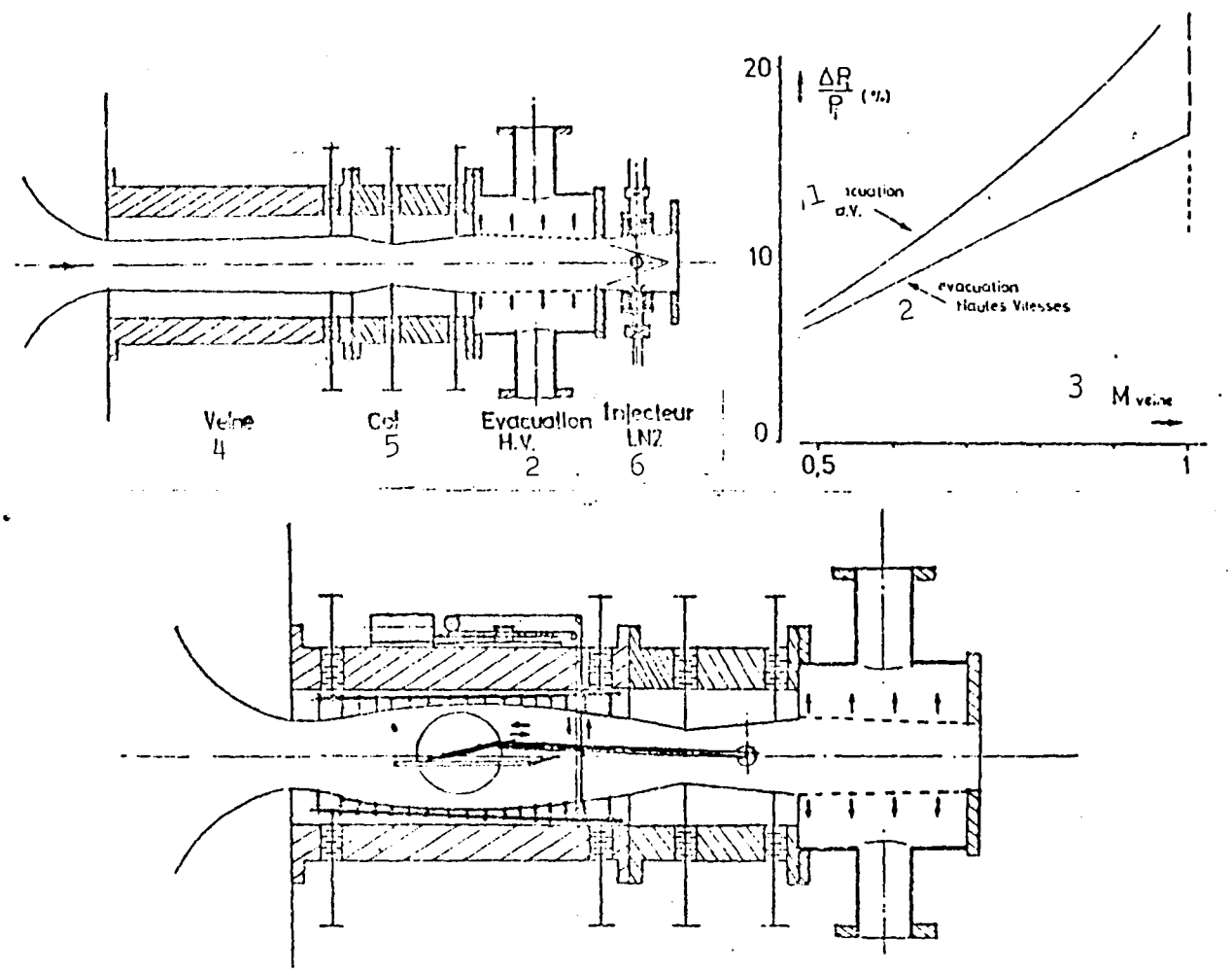

T'3 wind tunnel

THIS PAGE BLANK

REFERENCES

TECHNICAL REPORTS

J.C. JUILLEN et J. TRIAY

"Mesures de frottement pariétal par jauges à fil chaud sur profil LC 90 D (X = 1,4) à F1".

. R.T OA n° 52/2259 AND (DERAT n° 36/5004 DN) - Novembre 1982.

A. BLANCHARD et M.J. PAYRY

"Comportement de capteurs de pression miniaturisés à basse température. Etalonnage et utilisation dans une soufflerie cryogénique".

.R.T. OA n° 17/5007 AND (DERAT n° 17/5007 DN) - Novembre 1982.

M. OLIVE et A. BLANCHARD

"Etude expérimentale du déclenchement de la transition par des cavités en écoulement incompressible".

. R.T. OA N° 18/5007 AND (DERAT n° 18/5007 DN) - Décembre 1982.

J.P. ARCHAMBAUD

"Calcul de l'évolution du champ des températures dans un élément d'acier paroi-raidisseur au cours d'une rafale cryogénique".

. R.T. OA n° 23/5075 AND (DERAT n° 8/5015 DN) - Décembre 1982.

J.B. DOR et M. PLAZANET

"Approfondissement de l'étude expérimentale sur aile en flèche de profil. LC 100 D".

.R.T. OA n° 58/7078 AND (DERAT n° 8/5017 DN) - Décembre 1982.

J. COUSTEIX et R. HOUDEVILLE

"Couches limites instationnaires"

. R.T. OA n° 53/2259 AND (DERAT n° 37/5004 DN) - Janvier 1983.

J.L. BONNET et C. GLEYZES

"Etude expérimentale de la transition dans les bulbes de décollement laminaire au bord d'attaque des profils d'aile".

. R.T. OA n° 23/5018 AND (DERAT n° 23/5018 DN) - Janvier 1983.

D. ARNAL et C. GLEYZES

"Transition de la couche limite"

. RSF OA n° 24/5018 AYD (DERAT n° 24/5018 DY) - Janvier 1983.

C. GLEYZES et R. HOUDEVILLE

"Couches limites des turbomachines".

. RSF n° 9/5014 DN - Janvier 1983.

A. BLANCHARD

"Mise au point et utilisation de soufflerics cryogéniques".

. RSF OA n° 19/5007 AYD (DERAT n° 19/5007 DY) - Janvier 1983.

J. COUSTEIX

"Ecoulements turbulents tridimensionnels".

. RTS OA n° 54/2259 AYD (DERAT n° 38/5004 DY) - Mars 1983.

V. PIMONT

"Equations d'une couche limite turbulente épaisse sur un corps axisymétrique de section variable".

. RT OA n° 55/2259 AND (DERAT n° 39/5004 DN) - Mars 1983.

V. PIMONT

"Calcul de couches limites turbulentes épaisses et axisymétriques en fluide incompressible".

. RT OA n° 56/2259 AND (DERAT n° 40/5004 DN) - Mars 1983.

J.L. GOBERT et J.F. BREIL

"Etude préliminaire d'un dispositif de contrôle de la température de l'écoulement destiné à la soufflerie cryogénique T2".

. RT OA n° 20/5007 AND (DERAT n° 20/5007 DN) - Avril 1983.

X. de SAINT VICTOR et J. COUSTEIX

"Calcul de l'écoulement au voisinage du bord de fuite d'une plaque plane"

. R.T. OA n° 57/2259 AND (DERAT n° 41/5004 DN) - Août 1983.

X. de SAINT VICTOR et J. COUSTEIX

"Calcul du mélange tridimensionnel d'un sillage et d'une couche limite se développant dans des plans orthogonaux".

. R.T. OA n° 58/2259 AND (DERAT n° 42/5004 DN) - Août 1983.

J.B. DOR, A. MIGNOSI, M. PLAZANET

"Qualification de la soufflerie T2 en fonctionnement cryogénique :
A) Champ thermique - Etude préliminaire d'une maquette schématique"

. R.T. OA n° 24/5006 AND (DERAT N° 24/5006 DN) - Août 1983

J.B. DOR, A. MIGNOSI, M. PLAZANET

"Qualification de la soufflerie T2 en fonctionnement cryogénique :
B) Fluctuations de l'écoulement - détection et qualification de particules.

. R.T. OA n° 25/5006 AND (DERAT n° 25/5006 DN) - Septembre 1983.

A. SERAUDIE, J.P. ARCHAMBAUD, M. PLAZANET

"Qualification des couches limites et du proche sillage d'un profil CAST 7 (essais à température ambiante dans la soufflerie T2).

. R.T. OA n° 55/1685 AND (DERAT n° 1/5019 DN) - Septembre 1983.

TECHNICAL PAPERS

J.L. BONNET et R. HOUDEVILLE

"Utilisation du logiciel de tracé HEWLETT-PACKARD sur 21 MX".

. Fiche Technique n° 2/82 - Octobre 1982.

J.P. ARCHAMBAUD et A. MIGNOSI

"Précisions complémentaires sur la méthode d'adaptation utilisée pour le profil CAST 7 (Février-Mars 1982).
- Détermination du Mach à l'infini".

. Fiche Technique n° 3/82 - Octobre 1982.

R. HOUDEVILLE et J. COUSTEIX

"Liste des programmes de calcul diffusés par le DERAT".

. Fiche Technique n° 1/83 - Mars 1983.

J. COUSTEIX et B. AUPOIX

"An integral method for calculating a three-dimensional turbulent wake".

. Fiche Technique n° 2/83 - Juin 1983.

J.C. JUILLEN

"Etalonnage de trois jauges bidirectionnelles à fils chauds pour la mesure du frottement pariétal en écoulement tridimensionnel".

. Fiche Technique n° 3/83 - Juillet 1983.

° COMMUNICATIONS, PUBLICATIONS

B. AUPOIX et J. COUSTEIX

"Analyse d'effets de rotation sur la turbulence".

. Communication au 19° Colloque d'Aérodynamique Appliquée, 8-10 Nov. 1982 à Marseille.

C. GLEYZES, J. COUSTEIX, J.L. BONNET

"Méthode de calcul des bulbes de décollement de bord d'attaque"

. Communication au Second Symposium on Numerical and Physical Aspects of Aerodynamic Flows, Long Beach, California, 17-20 Janv. 1983.

J. COUSTEIX, G. PAILHAS, B. AUPOIX

"Sillage turbulent tridimensionnel d'une aile en flèche"

. Communication au Second Symposium on Numerical and Physical Aspects of Aerodynamics Flows, Long Beach, California, 17-20 Janv. 1983.

. T.P. ONERA 1983-9.

J. COUSTEIX et R. HOUDEVILLE

"Couches limites turbulentes instationnaires ou tridimensionnelles"

. Communication au VKI Lecture Series sur les Ecoulements Turbulents Cisaillés, Rhode St Genèse (Belgique), du 28 Fév. au 4 Mars 1983.

B. AUPOIX et J. COUSTEIX

"Calculs de couche limite tridimensionnelle dans un compresseur".

. Communication au congrès AGARD sur les effets visqueux dans les turbomachines, Copenhague, du 1er au 3 Juin 1983.

. T.P. ONERA n° 1983-47.

R. MICHEL, J. COUSTEIX, R. HOUDEVILLE

"Couches limites turbulentes instationnaires".

. Communication au 9ème Congrès Canadien de Mécanique Appliquée, Saskatoon, (Canada) du 30 Mai au 3 Juin 1983.

. Publication dans CANCAM.

J.P. CHEVALLIER, A. MIGNOSI, J.P. ARCHAMBAUD, A. SERAUDIE

"Parois adaptables à T2. Principes, réalisation et quelques exemples de résultats bidimensionnels".

. Article dans la R.A. 1983-4.

B. AUPOIX, J. COUSTEIX, J. LIANDRAT

"Effets de la rotation sur une turbulence isotrope".

. Communication au 4ème Symposium on "Turbulent Shear Flows", Université de Karlsruhe (RFA) du 12 au 14 Sept. 1983.

. T.P. ONERA (à paraître).

A. MIGNOSI et J.B. DOR

"La soufflerie cryogénique à parois auto-adaptables T2 de l'ONERA/CERT"

. Communication au Symposium AGARD on "Wind Tunnels and Testing Techniques", Izmir (Turquie) du 26 au 29 Sept. 83.

. T.P. ONERA (à paraître).

E. COUSTOLS, D. ARNAL

"Instability theory and transition criteria in 3D flows".

. Communication à EUROVISC Working Party on "Transition in Boundary Layers", NLR, Amsterdam (Pays-Bas), 15 et 16 Sept. 1983.

E. COUSTOLS, D. ARNAL

"Applications to swept wings; effect of sweep angle on transtion and drag".

. Communication à EUROVISC Working Party on "Transition in Boundary Layers", NLR, Amsterdam (Pays-Bas), 15 et 16 Sept. 1983.

J.C. JUILLEN, E. COUSTOLS, D. ARNAL

"Experimental research on laminar boundary layer and transition on a swept wing (special study of instability stationary waves)".

. Communication à EUROVISC Working Party on "Transition in Boundary Layers", NLR, Amsterdam (Pays-Bas) 15 et 16 Sept. 1983.

° TECHNICAL DISCOURSES

J. COUSTEIX, D. ARNAL, X. DE SAINT VICTOR

"Etude numérique des écoulements de coin par résolution des équations de Navier-Stokes".

(22 Février 1983)

G. PAILHAS, J.C.JUILLEN, R. HOUDEVILLE

"Développement de techniques de mesures d'écoulements turbulents"

(26 Avril 1983)

° THESES

COUSTOLS Eric

"Stabilité et transition en écoulement tridimensionnel : cas des ailes en flèche"

. Thèse présentée à l'ENSAE en vue de l'obtention du diplôme de Dr-Ing., le 29 Juin 1983.

° E.N.S.A.E PROJECTS UPON COMPLETION OF STUDIES

BATTESTI Jean-Yves

"Méthode semi-elliptique de calcul d'écoulements visqueux"

(24 Juin 1983)

LIANDRAT Jacques

"Effet de la rotation sur la turbulence"

(28 Juin 1983)

SCHMIDT Philippe

"Transition des couches limites sur les ailes en flèche"

(28 Juin 1983)

TETU Marie-Hélène

"Calcul de couche limite avec couplage simultané"

(28 Juin 1983)

∘ STAGE I.N.S.A.

LEMAIRE Pascal et TENAUD Christian

"Etude expérimentale et théorique d'un écoulement au voisinage d'une jonction aile-fuselage".

. Stage effectué du 1er Avril au 30 Juin 1983.

∘ STAGES I.U.T.

HOGANT Serge

"Etalonnage et utilisation d'une jauge à fils chauds pour la mesure du frottement pariétal en écoulement tridimensionnel".

. Stage effectué du 5 Janvier au 18 Février 1983.

EVRARD Jean

"Etalonnage de jauges de frottement à fil chaud en écoulement compressible"

. Stage effectué du 14 Février au 1er Avril 1983.